`

Development of an Analytical Model for the Equivalent Temperature Field to Imitate the Thermal Autofrettage Induced Residual Stress Field in Cylinders

A Project Report Submitted in Partial Fulfilment of the Requirements for the Degree of

Bachelor of Technology

In

Mechanical Engineering

by

Indranuj Sharma (MEB19016)

Jyotish Prasad Lahe (MEB19036)

Ketupati Swargiary (MEB19045)

Under the guidance of,

Dr. S. M. Kamal,

Assistant Professor,

Department of Mechanical Engineering,

Tezpur University

DEPARTMENT OF MECHANICAL ENGINEERING

SCHOOL OF ENGINEERING

TEZPUR UNIVERSITY

JUNE 2023

`

DEPARTMENT OF MECHANICAL ENGINEERING

TEZPUR UNIVERSITY

TEZPUR JUNE 2023

CERTIFICATE

This is to certify that the report entitled "**Development of an Analytical Model for the Equivalent Temperature Field to Imitate the Thermal Autofrettage Induced Residual Stress Field in Cylinders**" by **Indranuj Sharma (Roll No. MEB19016), Jyotish Prasad Lahe (Roll No. MEB19036), Ketupati Swargiary (Roll No. MEB19045)** submitted in the Department of Mechanical Engineering at Tezpur University, Tezpur, during the academic year 2022-23, in partial fulfilment of the requirements for the Degree of Bachelor of Technology in Mechanical Engineering, is carried out under our guidance and supervision. The work contained in this report has not been submitted elsewhere for a Degree/Diploma/Certificate.

_____

(Project Supervisor)

Dr. S. M. Kamal

Assistant Professor

Department of Mechanical Engineering

`

TEZPUR UNIVERSITY

SCHOOL OF ENGINEERING
DEPARTMENT OF MECHANICAL ENGINEERING
NAPAAM, DIST: SONITPUR, PIN:784028
ASSAM, INDIA

CERTIFICATE

This is to certify that we have examined this report on **"Development of an Analytical Model for the Equivalent Temperature Field to Imitate the Thermal Autofrettage Induced Residual Stress Field in Cylinders"** and hereby approve it as a study carried out and presented in a manner required for its acceptance and fulfilment for the bachelor's degree in mechanical engineering for which it has been submitted by

Indranuj Sharma (Roll No. MEB19016)

Jyotish Prasad Lahe (Roll No. MEB19036)

Ketupati Swargiary (Roll No. MEB19045)

This approval does not necessarily accept every statement made, opinion expressed, or conclusion drawn as recorded in this report. It only signifies the acceptance of this report for which it has been submitted.

The Viva-Voće of above candidates of 8th semester B.Tech. (Mechanical Engineering) of their project has been held on …….... and found satisfactory.

…… …….

Head of Department Examiner

`

ACKNOWLEDGEMENT

On the onset, we would like to express our gratitude to Dr. S. M. Kamal for his assistance and guidance throughout the B. Tech Project. We are appreciative that he was willing to share his time and knowledge with us because his expertise and knowledge were invaluable to us. With Dr. Kamal's assistance, we were able to develop a comprehensive comprehension of the project's subject and a solid research methodology. He also provided us with insightful feedback on our research findings and helped us improve the calibre of our work. We are grateful for Dr. Kamal's encouragement and support, and we are certain that we would not have been able to conclude our project successfully without his assistance.

The current project work is a part of a funded research project by DRDO. Funding from the Armament Research Board, DRDO (Govt. of India) through grant ARMREB/ADMB/2021/234, project, 'Use of Thermal Autofrettage for Defence Application' is gratefully acknowledged.

Indranuj Sharma (Roll No. MEB19016)

Jyotish Prasad Lahe (Roll No. MEB19036)

Ketupati Swargiary (Roll No. MEB19045)

`

ABSTRACT

To imitate autofrettage-induced residual stresses, the evaluation of equivalent temperature fields for cylindrical and spherical pressure vessels have been successfully implemented in studying crack growth in autofrettaged vessels by the finite element method. Thermal autofrettage is a potential alternative method for strengthening hollow cylinders used in high pressure application. In this work, an equivalent thermal loading approach is used in the finite element analysis to replicate the original thermal autofrettage-induced residual stress field. An analytical model for the equivalent temperature field for an arbitrary axisymmetric residual stress field induced in a thick-walled cylinder is developed. The analytical model is implemented in a finite element method analysis to reproduce the original thermal autofrettage-induced residual stresses in a thick-walled cylinder. The residual stress field obtained by applying the equivalent temperature field in the finite element method analysis are corroborated with the original residual stress field introduced by thermal autofrettage in the cylinder. It is found that the developed equivalent temperature fields can reproduce the residual stress fields induced by thermal autofrettage with reasonable accuracy.

`

Table of Contents

`

`

List of Tables

`

List of Figures

`

Chapter 1

Introduction

1.1 The Autofrettage Process

Autofrettage is a metal working process which is commonly practiced in industries for thick-walled cylindrical or spherical pressure vessels to increase their elastic load carrying capacity and service life. The barrel of a gun, vessels used in oil and chemical industries, high pressure pipelines, space shuttles, submarine hauls and nuclear reactors are some of the worth noting examples where autofrettage is employed. In autofrettage process the cylinder or sphere to be autofrettaged is initially subjected to a uniformly applied load causing non-homogeneous plastic deformation at the inner bore region of the component and certain portion beneath it. This stage is the loading stage as shown schematically in Fig. 1.1 (a). The material at and around the outer region of the cylinder or sphere remains elastic in the loading stage. As shown in Fig. 1.1 (a), a cylinder or sphere of inner radius *a* and outer radius *b* becomes plastic up to radius c forming the inner plastic region $a \leq r \leq c$ and outer elastic region $c \leq r \leq b$. In a later stage upon attaining a desired level of plastic deformation at the inner region of the cylinder or sphere, the plastically deforming load is removed. This is the unloading stage. After performing the unloading stage, the inner plastically deformed region tries to remain in its deformed state, whilst the outer elastically deformed region tries to spring back to its initial position. This counteraction produces compressive residual stresses of high magnitude at the inner bore region of the thick-walled cylinder or sphere. Due to self-equilibrating nature of the residual stresses, the outer region of the cylinder or sphere wall have tensile residual stresses, which are usually much lower in magnitude than the compressive residual stress at the inner region. The state of the cylinder after unloading is schematically shown in Fig. 1.1 (b). Once the compressive residual stresses are set up in the cylinder or sphere, the autofrettage procedure is said to be completed. The beneficial compressive residual stresses at the inner region and in its neighbourhood reduces the working stress level in the cylinder or sphere, when it is put in service in the next loading phase. Thus, the pressure carrying capacity of the cylinder or sphere is

`

increased. Further, the compressive residual stress suppresses the inner cracks at the inner side of the cylinder or sphere increasing its fatigue life.

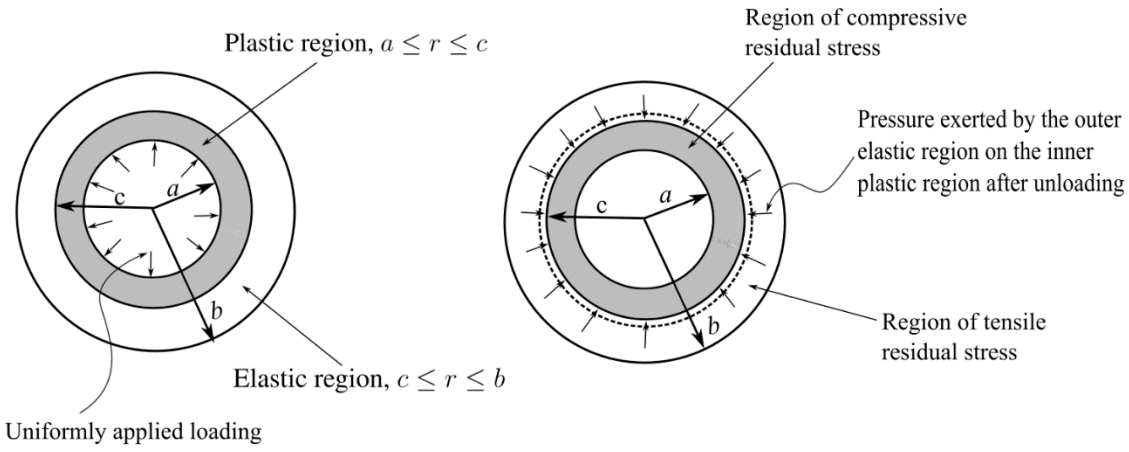

(a) (b)

Fig. 1.1 Schematic of autofrettage process: (a) Loading the cylinder/sphere, (b) state of the cylinder/sphere after unloading.

1.2 Evolution of Different Types of Autofrettage Processes

In 1907, Jacob, a French artillery officer, was the first person to examine the procedure of autofrettage with the purpose of pre stressing monobloc cannon barrels by internally pressurizing it [1]. This type of autofrettage process is popularly recognized as the hydraulic or pressure autofrettage. The process finds its first industrial application in French artillery industries around 1930 [2]. After five and half decades of the development of hydraulic autofrettage, Davidson et al. [3] originated and demonstrated the idea of achieving autofrettage by driving an extra-large mandrel through a thick-walled cylinder conceived, known as the swage autofrettage. In 1973, Ezra et al. [4] patented another method of achieving autofrettage, called explosive autofrettage. In explosive autofrettage process, an explosive charge is detonated at the inner bore region of the cylinder to achieve the intended level of plastic deformation. Both the hydraulic and swage autofrettage received significant attention of the researchers [5–8] and have been practiced in industries for long. However, the explosive autofrettage gain little attention due to involvement of explosives in its operation. Although the hydraulic and swage autofrettage processes have been practicing in industries for long, they pose certain

`

disadvantages. In case of hydraulic autofrettage, a great deal of caution is required when applying extremely high hydraulic pressure as this pressure needs to be precisely managed in order to accomplish the correct degree of deformation. The procedure is skill intensive, expensive, and may occasionally put the operator in danger. A significant amount of friction occurs between the mandrel and the inner surface of the cylinder during swage autofrettage with the requirement of a large amount of mandrel force. In order to avoid the disadvantages posed by the hydraulic and swage autofrettage processes, Kamal and Dixit [9] proposed a new method of thermal autofrettage process recently. The process can be achieved by loading and unloading of an induced radial temperature difference between the outer and inner wall of a thick-walled cylinder. The process does not require any hydraulic pressure for its operation and no friction is involved. Another recently proposed method is rotational autofrettage, conceived by Zare and Darijani [10]. In rotational autofrettage, the cylinder is first rotated at significantly high angular velocity and then it is brought to a complete stop to produce beneficial compressive residual stresses. As the present work addresses an important aspect of imitating residual stress field induced in thermal autofrettage of a cylinder in terms of an equivalent temperature field, a brief introduction to thermal autofrettage is provided in Section 1.3.

1.3 A Brief Introduction to Thermal Autofrettage

Thermal autofrettage method is based on the elastoplastic deformation of thick-walled cylinder caused by thermal stresses generated due to the temperature difference between the outer and inner wall of a thick-walled cylinder. The temperature difference in the cylinder required to achieve thermal autofrettage can be generated by heating the outer wall and cooling the inner wall simultaneously. A schematic of thermal autofrettage is shown in Fig. 1.2. As shown in Fig. 1.2, electric heating is employed to the outer wall of the cylinder to maintain a certain higher temperature T_b of the outer wall. Simultaneously, chilled water mixed with coolant is continuously regulated to keep the inner wall at sufficiently low temperature T_a. Thus, a temperature difference (T_b–T_a) that deforms the inner wall of the cylinder plastically up to a certain intermediate radius is created. The outer portion of the cylinder wall deforms elastically. Upon achieving the intended level of plastic deformation, the cylinder is allowed to cool to room temperature. This vanishes the temperature difference (T_b–T_a) in the cylinder and completes the operation of thermal autofrettage. At this stage, the inner region of the cylinder wall spread with compressive residual stresses.

`

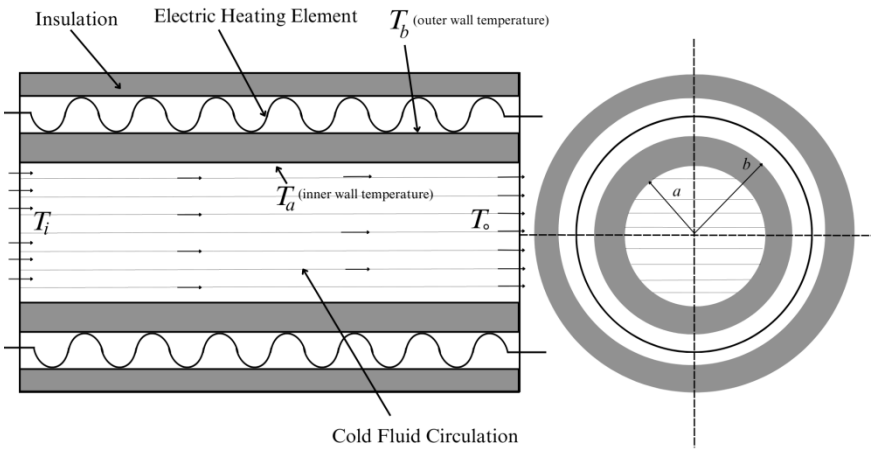

Fig. 1.2 A schematic of thermal autofrettage process [11]

1.4 Objective of the Present Work

One of the design tasks for the high pressure vessels is to suppress the inner cracks emanating from the inner side of the cylinder. This is very important to increase the service life of the cylinder. This can be achieved by means of autofrettage induced compressive residual stresses. To study the crack growth in cylinders in the presence of residual stresses, the crack tip stress intensity factors can be conveniently evaluated by using finite element method (FEM) analysis. It is worth mentioning that one of the possible ways to simulate the residual stress field in FEM analysis for the purpose of studying crack growth is by means of an equivalent temperature field [12]. The method of using equivalent temperature field is successfully implanted in a finite element framework to represent the residual stress field for autofrettage processes other than the new thermal autofrettage process. In view of this, the objective of the present work is to develop an analytical model for the equivalent temperature field to imitate the original residual stress field in cylinders induced by thermal autofrettage.

1.5 Organization of the Report

The project report is organized as follows:

Chapter 1 provides an introduction to autofrettage process along with a brief discussion on thermal autofrettage process and primary objective of the present work.

Chapter 2 presents a comprehensive literature review related to the present work.

`

Chapter 3 presents the analytical model for the equivalent temperature field to imitate the original residual stress field in cylinders induced by thermal autofrettage.

Chapter 4 concludes the report.

`

`

Chapter 2

Literature Review

2.1 Introduction

In this chapter a comprehensive review of literature related to the subject matter of the current project work is presented. The focus of the present project is to obtain an analytical solution of equivalent temperature field to reproduce the original thermal autofrettage induced residual stress field in cylinders. Autofrettage is a metal forming process widely employed in the design of many important engineering components, *e.g.*, pressure vessels, gun barrels, space shuttles, submarine hauls and fuel injection lines in diesel engines. There are five autofrettage processes are known in the literature, *viz.*, hydraulic, swage, explosive, thermal and rotational autofrettage processes. The age old hydraulic and swage autofrettage processes have been used in industries for long and investigated by a number of researchers [5–8, 13–20]. The explosive autofrettage although proposed as an alternative procedure by Ezra et al. [4], however, the process could not receive much attention as it involves explosive charge for its operation. The new thermal autofrettage [9, 21–23] is a promising technique providing certain operational benefits over the age-old methods. The recently proposed rotational autofrettage have been theoretically investigated by a few researchers [24–27]. In Section 2.2, a review of literature on thermal autofrettage is carried out followed by the review of literature on using the equivalent temperature field in FEM crack propagation analysis in Section 2.3.

2.2 Literature Review on Thermal Autofrettage

Thermal autofrettage is a recent development in the area of autofrettage. The process is based on the generation of compressive residual stresses by inducing a radial temperature difference across the wall thickness of a thick-walled cylinder. The first work on thermal autofrettage was reported by Kamal and Dixit [9]. They developed the closed-form analytical solutions for the stresses and strains in thermal autofrettage of a thick-walled cylinder using generalized plane strain condition, Tresca yield criterion and its

`

associated flow rule. A plane stress model of thermal autofrettage was also developed by Kamal and Dixit [21] using Tresca yield criterion and its associated flow rule incorporating strain hardening.

The first experimental work on thermal autofrettage was reported by Kamal et al. [22]. They experimentally verified the residual stresses in thermal autofrettage [9] using three different methods, *viz.*, Sachs boring, microhardness test and split ring method in SS304 and mild steel cylinders. Kamal et al. [23] also validated the residual stresses induced by thermal autofrettage in SS202 cylinders.

A comparative study of thermal autofrettage with the conventional hydraulic autofrettage was carried out by Kamal and Dixit [28]. They reported that although the hydraulic autofrettage is superior to thermal autofrettage in increasing the pressure carrying capacity of cylinders as compared to new thermal autofrettage process; the thermal autofrettage provides advantage when the cylinder has to work against radial temperature gradient. The thermal autofrettage is simple to operate and does not involve any ultra-high hydraulic pressure or explosives. Prima facie, the process is economical and a greener manufacturing procedure. In order to enhance further increase in the pressure carrying capacity of the thermally autofrettaged cylinder, the process was studied combining with shrink-fit by Kamal and Dixit [29]. It was found that the thermal autofrettage combined with shrink-fit provides significant enhancement in the pressure carrying capacity of the cylinder, which is of the order of 66% for wall thickness ratio 4 than that achieved in a thermally autofrettaged monobloc cylinder. The fatigue life enhancement of thermal autofrettage combined with shrink-fit was studied by Kamal and Dixit [30] using Paris fatigue crack-growth model.

A three-dimensional finite element method (FEM) modelling of thermal autofrettage of thick walled cylinders was carried out by Kamal et al. [31]. They obtained the solutions of stresses and compared with the theoretical plane stress and generalized plane strain model for different length to wall thickness ratios of the cylinder. Hence, they developed a criterion for the applicability of the theoretical plane stress and generalized plane strain model based on the length to wall thickness ratio of the cylinders. It was reported that the plane stress model is valid for cylinders with length to wall thickness ratio less than or equal to 1 and the generalized plane strain model is valid for cylinders

`

with length to wall thickness ratios more than or equal to 6. A detailed theoretical and experimental study of thermal autofrettage process can be found in Ref [32].

Shufen and Dixit [33] carried out a finite element method analysis of thermal autofrettage combined with conventional hydraulic autofrettage. They found that the pressure required to achieve autofrettage in the hybrid process is significantly reduced than that required in standalone hydraulic autofrettage process. In a later work, Shufen and Dixit [34] studied thermal autofrettage coupled with heat treatment. They found that the thermal autofrettage coupled with heat treatment creates compressive residual stresses even at the outer wall. This will help in resisting stress corrosion cracking of the cylinder significantly. Shufen et al. [35] also developed an experimental set up similar to Kamal et al. [22] coupled with heat treatment. They also verified the procedure using qualitative techniques based on microhardness test and split-ring method. Very recently, Rajput et al. [36] carried out an analytical study of thermal autofrettage of hollow disk by incorporating von Mises yield criterion.

2.3 Literature Review on Using the Equivalent Temperature Field in FEM Analysis

A number of researchers have used equivalent temperature field to predict the original autofrettage induced residual stress field. Some worth noting works are discussed below.

Hill [37] predicted an ideal residual stress field for the case of a fully autofrettaged cylindrical pressure vessel and this residual stress field was exactly replicated by an analytical expression for the axisymmetric temperature field obtained by Parker and Farrow [38]. Hussain et al. [12] proposed a derivation of thermal loading for simulating the partially autofrettaged case of a cylindrical vessel based on the analytical solution of Hill [37]. Pu and Hussain [12] successfully implemented this foregoing temperature field in an FEM model of a partially autofrettaged vessel with multiple cracks. They found that the redistribution of the residual stress field when a crack appears in the vessel can also be simulated by the equivalent temperature field.

Perl [40] evaluated the equivalent temperature field by proposing an exact numerical algorithm for any given analytical or numerical residual stress field induced by autofrettage in cylindrical pressure vessels. The equivalence of thermal loading and autofrettage residual stress for thick-walled spherical pressure vessels is also demonstrated by Perl [41] by presenting a similar methodology. This methodology is also

`

used by Perl and Arone [42] to simulate Hill's autofrettage-induced residual stress field in analysing stress intensity factors for a radially multi-cracked autofrettaged pressurized thick-walled cylinder.

For the finite element analysis of cracked spherical pressure vessels, Perl and Steiner [43, 44] applied the methodology of equivalent temperature field. The methodology of equivalent temperature field is used by de Swardt et al. [45] to simulate crack compliance experiments using FEM analysis in order to measure residual stresses in thick-walled cylinders. To imitate the residual stress field in a thick-walled autofrettaged pressure vessel, Güven [46] performed a theoretical analysis for the equivalent temperature loading based on the unified strength criterion, including the intermediate principal stress and the different strength effects, both in tension and in compression.

Recently, Perl et al. [47] used finite element method to emulate the rotational-autofrettage induced residual stresses by employing the equivalent temperature field in the FEM model of a rotating disk. They demonstrated the procedure for a rotating hollow SS304 disk subjected to rotational autofrettage and showed that the equivalent temperature field correctly reproduce the original rotational autofrettage induced residual stress field in the disk.

2.4 Research Gaps and Objectives

It is revealed from the literature review that the thermal autofrettage is an alternative potential process to increase the pressure carrying capacity and fatigue life of thick-walled cylindrical vessels. The process has been investigated both theoretically and experimentally by a few researchers. Quite a number of studies investigated the pressure carrying capacity of thermally autofrettaged cylinders. However, there are limited studies on the beneficial aspects of suppressing inner cracks due to thermal autofrettage induced residual stresses and evaluation of fatigue life. One of the best possible ways to study the beneficial aspect of crack propagation in autofrettaged cylinders is the use of equivalent temperature field emulating the autofrettage induced residual stresses in a numerical framework using finite element method. A number of researchers have used equivalent temperature field to study this beneficial aspect in other methods of autofrettage processes including new rotational autofrettage employed in disk. However, so far there is no study on the use of an equivalent temperature field to imitate the residual stresses originally

`

induced by the method of thermal autofrettage. Apart from this, there are also scopes in the refinement of the analytical modelling of thermal autofrettage incorporating more realistic yield criterion such as von Mises yield criterion.

In view of the research gaps identified above, in the present project work, it is proposed to work on the evaluation of equivalent temperature field to imitate the residual stresses in cylinders due to thermal autofrettage. The primary objective of this project is to develop an analytical model for the equivalent temperature field to imitate the thermal autofrettage induced residual stress field in cylinders. The closed from analytical solution is exemplified for a typical thermally autofrettaged SS304 cylinder. For this, the equivalent temperature field is applied in a finite element model in ABAQUS and then corroborated with the analytical solutions of thermal autofrettage residual stresses available in literature.

2.5 Conclusions

A literature review is carried out on thermal autofrettage and on the use of an equivalent temperature field imitating the autofrettage induced residual stresses. The research gaps are identified from the literature review. Based on the identified research gaps, the objective of the present work is decided. It is proposed to develop an analytical model for the equivalent temperature field for replicating the residual stresses induced in cylinders as a result of thermal autofrettage.

`

`

Chapter 3

An Analytical Model for the Equivalent Temperature Field to Imitate the Thermal Autofrettage Induced Residual Stress Field in Cylinders

3.1 Introduction

In this chapter, a methodology for emulating the residual stress field in a long thick-walled cylinder induced by thermal autofrettage is developed by establishing equivalence between the thermal stress field and the thermal autofrettage analytical or numerical residual stress fields. A closed-form analytical model is developed for evaluating the equivalent temperature field that reproduces the residual stress field in a cylinder subjected to thermal autofrettage using Kamal and Dixit's model [9]. The developed analytical model is numerically exemplified for a typical thermally autofrettaged cylinder by performing FEM analysis. This involves applying the equivalent temperature fields evaluated from the analytical model to the hollow cylinder in ABAQUS finite element framework and reproducing the corresponding residual stresses as originally induced by thermal autofrettage.

3.2 Mechanics of Thermal Autofrettage

For emulating the thermal autofrettage induced residual stress field by means of equivalent temperature field, it is important to understand the mechanics of thermal autofrettage. Here, the mechanics of thermal autofrettage developed by Kamal and Dixit [9] is briefly described.

3.2.1 States of plastic deformation in cylinder during thermal autofrettage

In a thick-walled long cylinder with free ends under radial temperature gradient, the steady-state temperature distribution is given by [48]

$$T = T_b + (T_a - T_b)\frac{\ln\left(\frac{b}{r}\right)}{\ln\left(\frac{b}{a}\right)}, \tag{3.1}$$

`

where a and b are the inner and outer radii of the cylinder, and T_a and T_b are the inner and outer wall temperatures.

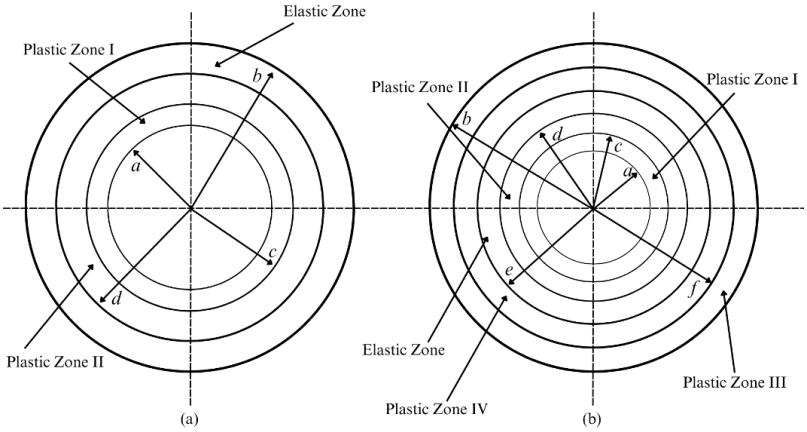

Fig. 3.1 (a) First and (b) second stage of plastic deformation with different plastic and elastic zones in thermally autofrettaged cylinder [9]

When the cylinder is loaded with a radial temperature difference, there are three situations of deformation occuring in the wall of the cylinder. The cylinder wall remains elastic if the temperature difference is below a certain first threshold, which is the yield onset temperature difference of the cylinder. Once it exceeds the first threshold temperature difference as per Tresca criterion, the inner wall of the cylinder is subjected to plastic deformation two consecutive plastic zones, *viz*., $a \leq r \leq c$ and $c \leq r \leq d$. The zone, $d \leq r \leq b$ at the outer portion of the cylinder wall deforms elastically. This situation of deformation is referred as the first stage of plastic deformation as depicted in Fig. 3.1 (a). Further, if the temperature difference is allowed to reach a certain second threshold, yielding initiates at the outer wall of the cylinder as well. Upon exceeding the second threshold temperature difference, the cylinder wall is formed with two more consecutive plastic zones propagating radially inwards from the outer wall, *viz*., $f \leq r \leq b$ and $e \leq r \leq f$ apart from the two inner plastic zones formed in the first stage of plastic deformation. The intermediate zone, $d \leq r \leq e$ remains in the elastic state. This situation of deformation is referred as the second stage of plastic deformation as shown in Fig. 3.1 (b). The radii d and e are called as the elastic-plastic interface radii. In a later stage, when the temperature difference is vanished by cooling the cylinder to room temperature, beneficial compressive residual stresses are set up at the inner side of the cylinder along with tensile residual stresses towards the outer wall of the cylinder. The detailed derivation of the thermal stresses induced in the cylinder when loaded with a plastically deforming

`

temperature difference as well as the post-unloading residual stresses induced in the first and second stage of plastic deformation can be found in Ref [9]. Nevertheless, for maintaining flow of this chapter, the equations developed in Ref [9] are cited here. The analysis is based on generalized plane strain condition, Tresca yield criterion and its associated flow rule.

3.2.2 Loading stresses in the first stage of elasto-plastic deformation

Plastic zone I: $a \le r \le c$

$$\sigma_r = k_1\sigma_Y \ln r + C_3, \tag{3.2}$$

$$\sigma_\theta = \sigma_z = k_1\sigma_Y \left(1+\ln r\right) + C_3. \tag{3.3}$$

Plastic zone II: $c \le r \le d$

$$\sigma_r = C_5 r^{-1+\sqrt{2(1-\nu)}} + C_6 r^{-1-\sqrt{2(1-\nu)}} + \frac{k_1\sigma_Y}{(2\nu-1)} + \frac{E\alpha T_a}{(2\nu-1)} + \frac{E\alpha\left(T_b-T_a\right)}{(2\nu-1)\ln\left(\frac{b}{a}\right)}\left\{\ln\left(\frac{r}{a}\right) - \frac{2\nu+1}{2\nu-1}\right\} - \frac{E\varepsilon_0}{(2\nu-1)}, \tag{3.4}$$

$$\sigma_\theta = C_5\sqrt{2(1-\nu)}\, r^{\sqrt{2(1-\nu)}-1} - C_6\sqrt{2(1-\nu)}\, r^{-\sqrt{2(1-\nu)}-1} + \frac{k_1\sigma_Y}{(2\nu-1)} + \frac{E\alpha T_a}{(2\nu-1)} + \frac{E\alpha\left(T_b-T_a\right)}{(2\nu-1)\ln\left(\frac{b}{a}\right)}\left\{\ln\left(\frac{r}{a}\right) - \frac{2}{2\nu-1}\right\} - \frac{E\varepsilon_0}{(2\nu-1)}. \tag{3.5}$$

$$\sigma_z = C_5 r^{-1+\sqrt{2(1-\nu)}} + C_6 r^{-1-\sqrt{2(1-\nu)}} + \left(\frac{2\nu}{2\nu-1}\right)k_1\sigma_Y + \frac{E\alpha T_a}{(2\nu-1)} + \frac{E\alpha\left(T_b-T_a\right)}{(2\nu-1)\ln\left(\frac{b}{a}\right)}\left\{\ln\left(\frac{r}{a}\right) - \frac{2\nu+1}{2\nu-1}\right\} - \frac{E\varepsilon_0}{(2\nu-1)}. \tag{3.6}$$

`

Elastic zone: $d \le r \le b$

$$\sigma_r = \frac{E\alpha}{2(1-\nu)}\frac{(T_b - T_a)}{\ln\left(\frac{b}{a}\right)}\left[\ln\left(\frac{b}{r}\right) - \left\{\frac{d^2}{b^2 + d^2(2\nu-1)}\right\}\left\{\ln\left(\frac{b}{a}\right)(2\nu-1) - \nu - \ln\left(\frac{d}{a}\right)\right\}\left(1-\frac{b^2}{r^2}\right)\right]$$
$$+\left\{\frac{d^2}{b^2 + d^2(2\nu-1)}\right\}k_1\sigma_Y\left(1-\frac{b^2}{r^2}\right) + \left\{\frac{d^2}{b^2 + d^2(2\nu-1)}\right\}E\alpha T_a\left(1-\frac{b^2}{r^2}\right) \quad (3.7)$$
$$-\left\{\frac{d^2}{b^2 + d^2(2\nu-1)}\right\}E\varepsilon_0\left(1-\frac{b^2}{r^2}\right),$$

$$\sigma_\theta = \frac{E\alpha}{2(1-\nu)}\frac{(T_b - T_a)}{\ln\left(\frac{b}{a}\right)}\left[\ln\left(\frac{b}{r}\right) - 1 - \left\{\frac{d^2}{b^2 + d^2(2\nu-1)}\right\}\left\{\ln\left(\frac{b}{a}\right)(2\nu-1) - \nu - \ln\left(\frac{d}{a}\right)\right\}\left(1+\frac{b^2}{r^2}\right)\right]$$
$$+\left\{\frac{d^2}{b^2 + d^2(2\nu-1)}\right\}k_1\sigma_Y\left(1+\frac{b^2}{r^2}\right) + \left\{\frac{d^2}{b^2 + d^2(2\nu-1)}\right\}E\alpha T_a\left(1+\frac{b^2}{r^2}\right)$$
$$-\left\{\frac{d^2}{b^2 + d^2(2\nu-1)}\right\}E\varepsilon_0\left(1+\frac{b^2}{r^2}\right),$$

(3.8)

$$\sigma_z = \frac{E\alpha\nu}{2(1-\nu)}\frac{(T_b - T_a)}{\ln\left(\frac{b}{a}\right)}\left[2\ln\left(\frac{b}{r}\right) - 1 - \left\{\frac{2d^2}{b^2 + d^2(2\nu-1)}\right\}\left\{\ln\left(\frac{b}{a}\right)(2\nu-1) - \nu - \ln\left(\frac{d}{a}\right)\right\}\right]$$
$$+\left\{\frac{2\nu d^2}{b^2 + d^2(2\nu-1)}\right\}k_1\sigma_Y + \left\{\frac{d^2 - b^2}{b^2 + d^2(2\nu-1)}\right\}E\alpha T_a - \left\{\frac{d^2 - b^2}{b^2 + d^2(2\nu-1)}\right\}E\varepsilon_0 \quad (3.9)$$
$$-E\alpha(T_b - T_a)\frac{\ln\left(\frac{r}{a}\right)}{\ln\left(\frac{b}{a}\right)}.$$

3.2.3 Loading stresses in the second stage of elasto-plastic deformation

Elastic zone: $d \le r \le e$

$$\sigma_r = \frac{E\alpha}{(2\nu-1)}T_a + \frac{E\alpha(T_b - T_a)}{2(1-\nu)\ln\left(\frac{b}{a}\right)}\left[\frac{1}{(2\nu-1)}\left\{\ln\left(\frac{d}{a}\right) + \frac{1}{2} - \frac{e^2}{2d^2}\right\} - \ln\left(\frac{r}{a}\right) + \frac{1}{2} - \frac{e^2}{2r^2}\right]$$
$$+\frac{k_1\sigma_Y}{2\nu-1}\left(1+\frac{e^2}{2d^2}\right) + \frac{e^2}{2r^2}k_1\sigma_Y + \frac{E\varepsilon_0}{(1-2\nu)}, \quad (3.10)$$

`

$$\sigma_\theta = \frac{E\alpha}{(2\nu-1)}T_a + \frac{E\alpha(T_b-T_a)}{2(1-\nu)\ln\left(\frac{b}{a}\right)}\left[\frac{1}{(2\nu-1)}\left\{\ln\left(\frac{d}{a}\right)+\frac{1}{2}-\frac{e^2}{2d^2}\right\}-\ln\left(\frac{r}{a}\right)-\frac{1}{2}+\frac{e^2}{2r^2}\right] + \frac{k_1\sigma_Y}{2\nu-1}\left(1+\frac{e^2}{2d^2}\right)-\frac{e^2}{2r^2}k_1\sigma_Y+\frac{E\varepsilon_0}{(1-2\nu)}. \tag{3.11}$$

$$\sigma_z = \frac{E\alpha}{(2\nu-1)}T_a + \frac{E\alpha(T_b-T_a)}{2(1-\nu)\ln\left(\frac{b}{a}\right)}\left[\frac{2\nu}{(2\nu-1)}\left\{\ln\left(\frac{d}{a}\right)+\frac{1}{2}-\frac{e^2}{2d^2}\right\}-2\ln\left(\frac{r}{a}\right)\right] + \frac{2\nu}{2\nu-1}k_1\sigma_Y\left(1+\frac{e^2}{2d^2}\right)+\frac{E\varepsilon_0}{(1-2\nu)}. \tag{3.12}$$

Plastic zone III: $f \le r \le b$

$$\sigma_r = -k_1\sigma_Y \ln r + C_7, \tag{3.13}$$

$$\sigma_\theta = \sigma_z = -k_1\sigma_Y(1+\ln r) + C_7, \tag{3.14}$$

Plastic zone IV: $e \le r \le f$

$$\sigma_r = \frac{E\alpha}{(2\nu-1)}T_a + \frac{E\alpha(T_b-T_a)}{2(1-\nu)\ln\left(\frac{b}{a}\right)}\left[\frac{1}{(2\nu-1)}\left\{\ln\left(\frac{d}{a}\right)+\frac{1}{2}-\frac{e^2}{2d^2}\right\}-\ln\left(\frac{e}{a}\right)\right] + k_1\sigma_Y\left\{\frac{1}{2\nu-1}\left(1+\frac{e^2}{2d^2}\right)+\frac{1}{2}-\ln\left(\frac{r}{e}\right)\right\}+\frac{E\varepsilon_0}{(1-2\nu)}. \tag{3.15}$$

$$\sigma_\theta = \frac{E\alpha}{(2\nu-1)}T_a + \frac{E\alpha(T_b-T_a)}{2(1-\nu)\ln\left(\frac{b}{a}\right)}\left[\frac{1}{(2\nu-1)}\left\{\ln\left(\frac{d}{a}\right)+\frac{1}{2}-\frac{e^2}{2d^2}\right\}-\ln\left(\frac{e}{a}\right)\right] + \left\{\frac{1}{2\nu-1}\left(1+\frac{e^2}{2d^2}\right)-\frac{1}{2}-\ln\left(\frac{r}{e}\right)\right\}k_1\sigma_Y+\frac{E\varepsilon_0}{(1-2\nu)}. \tag{3.16}$$

$$\sigma_z = \frac{E\alpha}{(2\nu-1)}T_a + \frac{E\alpha(T_b-T_a)}{2(1-\nu)\ln\left(\frac{b}{a}\right)}\left[\frac{2\nu}{(2\nu-1)}\left\{\ln\left(\frac{d}{a}\right)+\frac{1}{2}-\frac{e^2}{2d^2}\right\}+2\nu\ln\left(\frac{r}{e}\right)-2\ln\left(\frac{r}{a}\right)\right] + k_1\sigma_Y\left\{\frac{2\nu}{2\nu-1}\left(1+\frac{e^2}{2d^2}\right)-2\nu\ln\left(\frac{r}{e}\right)\right\}+\frac{E\varepsilon_0}{(1-2\nu)}. \tag{3.17}$$

`

The loading thermal stress solutions in the plastic zone I and II remain the same as in the first stage of elasto-plastic deformation. In the above equations k_1 is the sign factor that can be 1 or –1 depending on $T_b > T_a$ or $T_b < T_a$. In the present case, $T_b > T_a$ and hence k_1 =1.

3.2.4 Determination of various constants and unknown interface radii

In the equations cited in Sections 3.2.2 and 3.2.3, ε_0 is the constant axial strain and can be determined from the condition of generalized plane strain, *i.e.*, the total axial force is zero in each stage of elasto-plastic deformation. The different integration constants in the equations can be obtained employed appropriate boundary conditions. To determine constants, C_5 and C_6 the following boundary conditions are employed at $r=d$:

$$\sigma_r^{(\text{plastic zone II})} = \sigma_r^{(\text{elastic zone})}, \qquad \varepsilon_r^{p(\text{plastic zone II})} = 0. \tag{3.18}$$

The integration constant C_3 can be determined using the continuity of radial stress at the interface between the plastic zone I and II, *i.e.*, at $r=c$. Similarly, the use of the continuity of radial stress at the interface between the plastic zone III and IV, *i.e.*, at $r=f$ yields constant C_7. The resulting expressions of different constants are provided in Appendix.

To find out the values of radii c and d in the first stage of elasto-plastic deformation, the boundary conditions of vanishing radial stress at the inner radius and $\sigma_\theta^{(\text{plastic zone II})} = \sigma_z^{(\text{plastic zone II})}$ at $r=c$ are used. In the second stage of elasto-plastic deformation, radii c, d, e and f are evaluated by using the boundary conditions of vanishing radial stress at the inner and outer radii, $\sigma_\theta^{(\text{plastic zone II})} = \sigma_z^{(\text{plastic zone II})}$ at $r=c$ and $\sigma_\theta^{(\text{plastic zone IV})} = \sigma_z^{(\text{plastic zone IV})}$, at $r=f$.

3.2.5 The solution of residual stresses in thermal autofrettage

The residual thermal stresses are obtained by subtracting the pure thermoelastic stress solutions from the respective equations of radial, hoop and axial stresses in different zones for each stage of deformation. The solutions of residual stresses after unloading in the first and second stage of plastic deformation are provided as follows [9]:

`

3.2.5.1 Residual stresses induced in the first stage of plastic deformation

Plastic zone I, $a \le r \le c$

$$\left(\sigma_r\right)_{res} = k_1\sigma_Y \ln r + C_3 + \frac{E\alpha\left(T_b - T_a\right)}{2\left(1-\nu\right)\ln\left(\frac{b}{a}\right)}\left\{\ln\left(\frac{r}{a}\right) - \ln\left(\frac{b}{a}\right)\left(1-\frac{a^2}{r^2}\right)\frac{b^2}{b^2-a^2}\right\}, \tag{3.19}$$

$$\left(\sigma_\theta\right)_{res} = k_1\sigma_Y\left(1+\ln r\right) + C_3 + \frac{E\alpha\left(T_b - T_a\right)}{2\left(1-\nu\right)\ln\left(\frac{b}{a}\right)}\left\{1+\ln\left(\frac{r}{a}\right) - \ln\left(\frac{b}{a}\right)\left(1+\frac{a^2}{r^2}\right)\frac{b^2}{b^2-a^2}\right\}, \tag{3.20}$$

$$\left(\sigma_z\right)_{res} = k_1\sigma_Y\left(1+\ln r\right) + C_3 + \frac{E\alpha\left(T_b - T_a\right)}{2\left(1-\nu\right)\ln\left(\frac{b}{a}\right)}\left\{1+2\ln\left(\frac{r}{a}\right) - \ln\left(\frac{b}{a}\right)\frac{2b^2}{b^2-a^2}\right\}. \tag{3.21}$$

Plastic zone II, $c \le r \le d$

$$\begin{aligned}\left(\sigma_r\right)_{res} &= C_5 r^{-1+\sqrt{2(1-\nu)}} + C_6 r^{-1-\sqrt{2(1-\nu)}} + \frac{k_1\sigma_Y}{\left(2\nu-1\right)} + \frac{E\alpha T_a}{\left(2\nu-1\right)} + \frac{E\alpha\left(T_b-T_a\right)}{\left(2\nu-1\right)\ln\left(\frac{b}{a}\right)}\left\{\ln\left(\frac{r}{a}\right) - \frac{2\nu+1}{2\nu-1}\right\} \\ &- \frac{E\varepsilon_0}{\left(2\nu-1\right)} + \frac{E\alpha\left(T_b-T_a\right)}{2\left(1-\nu\right)\ln\left(\frac{b}{a}\right)}\left\{\ln\left(\frac{r}{a}\right) - \ln\left(\frac{b}{a}\right)\left(1-\frac{a^2}{r^2}\right)\frac{b^2}{b^2-a^2}\right\},\end{aligned} \tag{3.22}$$

$$\begin{aligned}\left(\sigma_\theta\right)_{res} &= C_5\sqrt{2\left(1-\nu\right)}r^{\sqrt{2(1-\nu)}-1} - C_6\sqrt{2\left(1-\nu\right)}r^{-\sqrt{2(1-\nu)}-1} + \frac{k_1\sigma_Y}{\left(2\nu-1\right)} + \frac{E\alpha T_a}{\left(2\nu-1\right)} + \frac{E\alpha\left(T_b-T_a\right)}{\left(2\nu-1\right)\ln\left(\frac{b}{a}\right)}\left\{\ln\left(\frac{r}{a}\right) - \frac{2}{2\nu-1}\right\} \\ &- \frac{E\varepsilon_0}{\left(2\nu-1\right)} + \frac{E\alpha\left(T_b-T_a\right)}{2\left(1-\nu\right)\ln\left(\frac{b}{a}\right)}\left\{1+\ln\left(\frac{r}{a}\right) - \ln\left(\frac{b}{a}\right)\left(1+\frac{a^2}{r^2}\right)\frac{b^2}{b^2-a^2}\right\},\end{aligned} \tag{3.23}$$

$$\begin{aligned}\left(\sigma_z\right)_{res} &= C_5 r^{-1+\sqrt{2(1-\nu)}} + C_6 r^{-1-\sqrt{2(1-\nu)}} + \left(\frac{2\nu}{2\nu-1}\right)k_1\sigma_Y + \frac{E\alpha T_a}{\left(2\nu-1\right)} + \frac{E\alpha\left(T_b-T_a\right)}{\left(2\nu-1\right)\ln\left(\frac{b}{a}\right)}\left\{\ln\left(\frac{r}{a}\right) - \frac{2\nu+1}{2\nu-1}\right\} - \frac{E\varepsilon_0}{\left(2\nu-1\right)} \\ &+ \frac{E\alpha\left(T_b-T_a\right)}{2\left(1-\nu\right)\ln\left(\frac{b}{a}\right)}\left\{1+2\ln\left(\frac{r}{a}\right) - \ln\left(\frac{b}{a}\right)\frac{2b^2}{b^2-a^2}\right\}.\end{aligned} \tag{3.24}$$

`

Elastic zone, $d \le r \le b$

$$(\sigma_r)_{res} = \frac{E\alpha}{2(1-\nu)}\frac{(T_b - T_a)}{\ln\left(\frac{b}{a}\right)}\left[\ln\left(\frac{b}{a}\right) - \ln\left(\frac{b}{a}\right)\left(1-\frac{a^2}{r^2}\right)\frac{b^2}{b^2-a^2} - \left\{\frac{d^2}{b^2+d^2(2\nu-1)}\right\}\left\{\ln\left(\frac{b}{a}\right)(2\nu-1) - \nu - \ln\left(\frac{d}{a}\right)\right\}\left(1-\frac{b^2}{r^2}\right)\right] \quad (3.25)$$
$$+\left\{\frac{d^2}{b^2+d^2(2\nu-1)}\right\}k_1\sigma_Y\left(1-\frac{b^2}{r^2}\right) + \left\{\frac{d^2}{b^2+d^2(2\nu-1)}\right\}E\alpha T_a\left(1-\frac{b^2}{r^2}\right) - \left\{\frac{d^2}{b^2+d^2(2\nu-1)}\right\}E\varepsilon_0\left(1-\frac{b^2}{r^2}\right),$$

$$(\sigma_\theta)_{res} = \frac{E\alpha}{2(1-\nu)}\frac{(T_b - T_a)}{\ln\left(\frac{b}{a}\right)}\left[\ln\left(\frac{b}{a}\right) - \ln\left(\frac{b}{a}\right)\left(1+\frac{a^2}{r^2}\right)\frac{b^2}{b^2-a^2} - \left\{\frac{d^2}{b^2+d^2(2\nu-1)}\right\}\left\{\ln\left(\frac{b}{a}\right)(2\nu-1) - \nu - \ln\left(\frac{d}{a}\right)\right\}\left(1+\frac{b^2}{r^2}\right)\right] \quad (3.26)$$
$$+\left\{\frac{d^2}{b^2+d^2(2\nu-1)}\right\}k_1\sigma_Y\left(1+\frac{b^2}{r^2}\right) + \left\{\frac{d^2}{b^2+d^2(2\nu-1)}\right\}E\alpha T_a\left(1+\frac{b^2}{r^2}\right) - \left\{\frac{d^2}{b^2+d^2(2\nu-1)}\right\}E\varepsilon_0\left(1+\frac{b^2}{r^2}\right),$$

$$(\sigma_z)_{res} = \frac{E\alpha}{2(1-\nu)}\frac{(T_b - T_a)}{\ln\left(\frac{b}{a}\right)}\left[1+2\ln\left(\frac{r}{a}\right) - \ln\left(\frac{b}{a}\right)\frac{2b^2}{b^2-a^2} + 2\nu\ln\left(\frac{b}{r}\right) - \nu - \left\{\frac{2\nu d^2}{b^2+d^2(2\nu-1)}\right\}\left\{\ln\left(\frac{b}{a}\right)(2\nu-1) - \nu - \ln\left(\frac{d}{a}\right)\right\}\right] \quad (3.27)$$
$$+\left\{\frac{2\nu d^2}{b^2+d^2(2\nu-1)}\right\}k_1\sigma_Y + \left\{\frac{d^2-b^2}{b^2+d^2(2\nu-1)}\right\}E\alpha T_a - \left\{\frac{d^2-b^2}{b^2+d^2(2\nu-1)}\right\}E\varepsilon_0 - E\alpha(T_b - T_a)\frac{\ln\left(\frac{r}{a}\right)}{\ln\left(\frac{b}{a}\right)}.$$

3.2.5.2 Residual stresses induced in the second stage of plastic deformation

The expressions of the residual stresses in the plastic zones I & II are given by Eqs. (3.19) – (3.24) only with the change of the values of the constants due to change of boundary conditions in the second stage of plastic deformation. The residual stresses in the elastic zone and two outer plastic zones are given as follows [9]:

Elastic zone, $d \le r \le e$

$$(\sigma_\theta)_{res} = \frac{E\alpha}{(2\nu-1)}T_a + \frac{E\alpha(T_b - T_a)}{2(1-\nu)\ln\left(\frac{b}{a}\right)}\left[\frac{1}{(2\nu-1)}\left\{\ln\left(\frac{d}{a}\right) + \frac{1}{2} - \frac{e^2}{2d^2}\right\} + \frac{1}{2} + \frac{e^2}{2r^2} - \ln\left(\frac{b}{a}\right)\left(1+\frac{a^2}{r^2}\right)\frac{b^2}{b^2-a^2}\right] \quad (3.28)$$
$$+\frac{k_1\sigma_Y}{2\nu-1}\left(1+\frac{e^2}{2d^2}\right) - \frac{e^2}{2r^2}k_1\sigma_Y + \frac{E\varepsilon_0}{(1-2\nu)},$$

$$(\sigma_z)_{res} = \frac{E\alpha}{(2\nu-1)}T_a + \frac{E\alpha(T_b - T_a)}{2(1-\nu)\ln\left(\frac{b}{a}\right)}\left[\frac{2\nu}{(2\nu-1)}\left\{\ln\left(\frac{d}{a}\right) + \frac{1}{2} - \frac{e^2}{2d^2}\right\} + 1 - \ln\left(\frac{b}{a}\right)\frac{2b^2}{b^2-a^2}\right] \quad (3.29)$$
$$+\frac{2\nu}{2\nu-1}k_1\sigma_Y\left(1+\frac{e^2}{2d^2}\right) + \frac{E\varepsilon_0}{(1-2\nu)}.$$

`

$$(\sigma_r)_{res}=\frac{E\alpha}{(2\nu-1)}T_a+\frac{E\alpha(T_b-T_a)}{2(1-\nu)\ln\left(\frac{b}{a}\right)}\left[\frac{1}{(2\nu-1)}\left\{\ln\left(\frac{d}{a}\right)+\frac{1}{2}-\frac{e^2}{2d^2}\right\}+\frac{1}{2}-\frac{e^2}{2r^2}-\ln\left(\frac{b}{a}\right)\left(1-\frac{a^2}{r^2}\right)\frac{b^2}{b^2-a^2}\right]$$
$$+\frac{k_1\sigma_Y}{2\nu-1}\left(1+\frac{e^2}{2d^2}\right)+\frac{e^2}{2r^2}k_1\sigma_Y+\frac{E\varepsilon_0}{(1-2\nu)}, \tag{3.30}$$

Plastic zone III, $f\le r\le b$

$$(\sigma_\theta)_{res}=-k_1\sigma_Y(1+\ln r)+C_7+\frac{E\alpha(T_b-T_a)}{2(1-\nu)\ln\left(\frac{b}{a}\right)}\left\{1+\ln\left(\frac{r}{a}\right)-\ln\left(\frac{b}{a}\right)\left(1+\frac{a^2}{r^2}\right)\frac{b^2}{b^2-a^2}\right\}, \tag{3.31}$$

$$(\sigma_z)_{res}=-k_1\sigma_Y(1+\ln r)+C_7+\frac{E\alpha(T_b-T_a)}{2(1-\nu)\ln\left(\frac{b}{a}\right)}\left\{1+2\ln\left(\frac{r}{a}\right)-\ln\left(\frac{b}{a}\right)\frac{2b^2}{b^2-a^2}\right\}. \tag{3.32}$$

$$(\sigma_r)_{res}=-k_1\sigma_Y\ln r+C_7+\frac{E\alpha(T_b-T_a)}{2(1-\nu)\ln\left(\frac{b}{a}\right)}\left\{\ln\left(\frac{r}{a}\right)-\ln\left(\frac{b}{a}\right)\left(1-\frac{a^2}{r^2}\right)\frac{b^2}{b^2-a^2}\right\}, \tag{3.33}$$

Plastic zone IV, $e\le r\le f$

$$(\sigma_\theta)_{res}=\frac{E\alpha}{(2\nu-1)}T_a+\frac{E\alpha(T_b-T_a)}{2(1-\nu)\ln\left(\frac{b}{a}\right)}\left[\frac{1}{(2\nu-1)}\left\{\ln\left(\frac{d}{a}\right)+\frac{1}{2}-\frac{e^2}{2d^2}\right\}+1+\ln\left(\frac{r}{e}\right)-\ln\left(\frac{b}{a}\right)\left(1+\frac{a^2}{r^2}\right)\frac{b^2}{b^2-a^2}\right]$$
$$+\left\{\frac{1}{2\nu-1}\left(1+\frac{e^2}{2d^2}\right)-\frac{1}{2}-\ln\left(\frac{r}{e}\right)\right\}k_1\sigma_Y+\frac{E\varepsilon_0}{(1-2\nu)}, \tag{3.34}$$

$$(\sigma_z)_{res}=\frac{E\alpha}{(2\nu-1)}T_a+\frac{E\alpha(T_b-T_a)}{2(1-\nu)\ln\left(\frac{b}{a}\right)}\left[\frac{2\nu}{(2\nu-1)}\left\{\ln\left(\frac{d}{a}\right)+\frac{1}{2}-\frac{e^2}{2d^2}\right\}+2\nu\ln\left(\frac{r}{e}\right)+1-\ln\left(\frac{b}{a}\right)\frac{2b^2}{b^2-a^2}\right]$$
$$+k_1\sigma_Y\left\{\frac{2\nu}{2\nu-1}\left(1+\frac{e^2}{2d^2}\right)-2\nu\ln\left(\frac{r}{e}\right)\right\}+\frac{E\varepsilon_0}{(1-2\nu)}. \tag{3.35}$$

$$(\sigma_r)_{res}=\frac{E\alpha}{(2\nu-1)}T_a+\frac{E\alpha(T_b-T_a)}{2(1-\nu)\ln\left(\frac{b}{a}\right)}\left[\frac{1}{(2\nu-1)}\left\{\ln\left(\frac{d}{a}\right)+\frac{1}{2}-\frac{e^2}{2d^2}\right\}+\ln\left(\frac{r}{e}\right)-\ln\left(\frac{b}{a}\right)\left(1-\frac{a^2}{r^2}\right)\frac{b^2}{b^2-a^2}\right]$$
$$+k_1\sigma_Y\left\{\frac{1}{2\nu-1}\left(1+\frac{e^2}{2d^2}\right)+\frac{1}{2}-\ln\left(\frac{r}{e}\right)\right\}+\frac{E\varepsilon_0}{(1-2\nu)}, \tag{3.36}$$

`

3.3 The Equivalent Temperature Field

In an axisymmetric hollow cylinder with inner radius *a* and outer radius *b*, the states of elastic stress due to generalized plane strain condition under steady state temperature field $T(r)$ are given by [49]

$$\sigma_{rr}(r) = -\frac{\alpha E}{(1-\nu)}\left(\frac{1}{r^2}\right)\int_a^r T(r)r\mathrm{d}r + \frac{E}{(1+\nu)}\left\{\frac{C_1}{(1-2\nu)} - \frac{C_2}{r^2}\right\}, \tag{3.37}$$

$$\sigma_{\theta\theta}(r) = \frac{\alpha E}{(1-\nu)}\left(\frac{1}{r^2}\right)\int_a^r T(r)r\mathrm{d}r - \frac{\alpha E T(r)}{(1-\nu)} + \frac{E}{1+\nu}\left\{\frac{C_1}{(1-2\nu)} + \frac{C_2}{r^2}\right\}, \tag{3.38}$$

where C_1 and C_2 are integration constants. Using the boundary conditions of vanishing radial stress at $r = a$ and $r = b$, the integration constants C_1 and C_2 can be evaluated by using the following boundary conditions:

$$\left(\sigma_r\right)\Big|_{r=a} = 0, \tag{3.39}$$

$$\left(\sigma_r\right)\Big|_{r=b} = 0. \tag{3.40}$$

Using Eqs. (3.39) and (3.40) and solving the resulting equations, the constants C_1 and C_2 are obtained as

$$C_1 = \frac{\alpha(1+\nu)(1-2\nu)}{(1-\nu)\left(b^2-a^2\right)}\int_a^b T(r)r\mathrm{d}r, \tag{3.41}$$

$$C_2 = \alpha\left(\frac{1+\nu}{1-\nu}\right)\frac{a^2}{b^2-a^2}\int_a^b T(r)r\mathrm{d}r. \tag{3.42}$$

Substituting Eqs. (3.41) and (3.42) in Eqs. (3.37) and (3.38), the resulting radial and hoop stress distribution as a function of temperature is obtained as

$$\sigma_{rr}(r) = \left(\frac{1}{1-\nu}\right)\frac{E\alpha}{r^2}\left\{\frac{r^2-a^2}{b^2-a^2}\int_a^b T(r)r\mathrm{d}r - \int_a^r T(r)r\mathrm{d}r\right\}, \tag{3.43}$$

$$\sigma_{\theta\theta}(r) = \left(\frac{1}{1-\nu}\right)\frac{E\alpha}{r^2}\left\{\frac{r^2+a^2}{b^2-a^2}\int_a^b T(r)r\mathrm{d}r + \int_a^r T(r)r\mathrm{d}r - T(r)r^2\right\}. \tag{3.44}$$

To evaluate the hoop stress at inner radius $r = a$, Eq. (3.44) can be rewritten in the following form providing definite integral as:

`

$$I_1 = \int_a^b T(r) r \mathrm{d}r = \sigma_{\theta\theta}(a)\left(\frac{b^2 - a^2}{2}\right)\left(\frac{1-\nu}{E\alpha}\right) + \left(\frac{b^2 - a^2}{2}\right)T(a)\,. \tag{3.45}$$

Adding Eqs. (3.43) and (3.44) yields

$$I_1 = (1-\nu)\left(\frac{b^2 - a^2}{2}\right)\frac{\sigma_{rr}(r) + \sigma_{\theta\theta}(r)}{E\alpha} + \left(\frac{b^2 - a^2}{2}\right)T(r)\,. \tag{3.46}$$

Comparing Eq. (3.45) with Eq. (3.46), the temperature field as a function of radial position is obtained as

$$T(r_i) = \left(\frac{1-\nu}{E\alpha}\right)\left\{\sigma_{\theta\theta}(a) - \sigma_{rr}(r_i) - \sigma_{\theta\theta}(r_i)\right\} + T(a)\,. \tag{3.47}$$

The analytical equivalent temperature field can be determined using Eq. (3.47) by substituting the distributions of residual thermal stress resulting from thermal autofrettage, $\sigma_{rr}(r_i)$ and $\sigma_{\theta\theta}(r_i)$. The equivalent temperature field so obtained can exactly replicate the residual stress distribution due to thermal autofrettage in cylinder. This amounts to an inverse estimation of the temperature field that causes a prior stress field.

3.3.1 Analytical solutions for the equivalent temperature field for a thermally autofrettaged cylinder subjected to first stage of plastic deformation

A cylinder subjected to thermal autofrettage undergoing first stage of plastic deformation is considered. The three zones, *viz*. plastic zone I, plastic zone II and elastic zone commences when the temperature difference crosses the first threshold as described in Section 3.2. In this case, the analytical solutions for the equivalent temperature field in different zones can be obtained by substituting the respective residual stress distributions in Eq. (3.47).

Using the residual stress distributions given by Eqs. (3.19) and (3.20) in Eq. (3.47), the solution for equivalent temperature field in the Plastic zone I, $a \le r \le c$ can be obtained as

$$T(r) = \left(\frac{1-\nu}{E\alpha}\right)\left\{k_1\sigma_Y \ln\left(\frac{a}{r^2}\right) + \frac{E\alpha\left(T_b - T_a\right)}{1-\upsilon}\frac{\ln\left(\frac{a}{r}\right)}{\ln\left(\frac{b}{a}\right)} - C_3\right\} + T_a. \tag{3.48}$$

`

Substitution of the expressions of residual radial and hoop stresses given by Eqs. (3.22) and (3.23) in Eq. (3.47) provides the solution for equivalent temperature field in the Plastic zone II, $c \le r \le d$ as

$$T(r)=\left(\frac{1-\nu}{E\alpha}\right)\left[\begin{array}{l} k_1\sigma_Y\left\{1+\ln(a)-\left(\frac{2}{2\nu-1}\right)\right\}+C_3-\frac{E\alpha(T_b-T_a)}{(1-\nu)\ln\left(\frac{b}{a}\right)}\ln\left(\frac{r}{a}\right)-C_5\left\{r^{\sqrt{2(1-\nu)}-1}\left(\sqrt{2(1-\nu)}+1\right)\right\} \\ -C_6\left\{r^{-\sqrt{2(1-\nu)}-1}\left(1-\sqrt{2(1-\nu)}\right)\right\}-\frac{2E\alpha T_a}{(2\nu-1)}-\frac{E\alpha(T_b-T_a)}{(2\nu-1)\ln\left(\frac{b}{a}\right)}\left\{\begin{array}{l}2\ln\left(\frac{r}{a}\right)- \\ \frac{3+2\upsilon}{2\upsilon-1}\end{array}\right\}+\frac{2E\varepsilon_o}{(2\nu-1)} \end{array}\right]+T_a. \quad (3.49)$$

Similarly, using Eqs. (3.25) and (3.26) in Eq. (3.47), the analytical expression of the equivalent temperature field for the elastic zone, $d \le r \le b$ is obtained as

$$T(r)=\left(\frac{1-\nu}{E\alpha}\right)\left[\begin{array}{l} k_1\sigma_Y\left\{1+\ln(a)\right\}+C_3 \\ +\frac{E\alpha(T_b-T_a)}{2(1-\nu)\ln\left(\frac{b}{a}\right)}\left\{\begin{array}{l}1-2\ln\left(\frac{b}{a}\right)+2\left\{\frac{d^2}{b^2+d^2(2\nu-1)}\right\} \\ \left\{\ln\left(\frac{b}{a}\right)(2\nu-1)-\nu-\ln\left(\frac{d}{a}\right)\right\}\end{array}\right\} \\ -\left\{\frac{2d^2}{b^2+d^2(2\nu-1)}\right\}\left(k_1\sigma_Y+E\alpha T_a-E\varepsilon_o\right) \end{array}\right]+T_a. \quad (3.50)$$

3.3.2 Analytical solutions for the equivalent temperature field for a thermally autofrettaged cylinder subjected to second stage of plastic deformation

During the second stage of plastic deformation in thermal autofrettage, there exists two additional plastic zones, Plastic zone III, $f \le r \le b$ and Plastic zone IV, $e \le r \le f$ at the outer wall of the cylinder with an intermediate zone $d \le r \le e$ as described in Section 3.2. Using the respective residual stress equations from Subsection 3.2.5.2 in Eq. (3.47), the analytical equivalent temperature field for replicating the original autofrettage induced residual stress distribution in the two outer plastic zones and in the intermediate elastic zone for the second stage of plastic deformation are obtained as follows:

`

Plastic zone III, $f \le r \le b$

$$T(r) = \left(\frac{1-\nu}{E\alpha}\right)\left[\begin{array}{l} k_1\sigma_Y\left(2+2\ln r+\ln a\right)+C_3-2C_7 \\ -\dfrac{E\alpha(T_b-T_a)}{(1-\nu)\ln\left(\dfrac{b}{a}\right)}\ln\left(\dfrac{r}{a}\right) \end{array}\right]+T_a \qquad (3.51)$$

Plastic zone IV, $e \le r \le f$

$$T(r) = \left(\frac{1-\nu}{E\alpha}\right)\left[\begin{array}{l} k_1\sigma_Y\left\{1+\ln(a)-\dfrac{2}{(2\nu-1)}\left(1+\dfrac{e^2}{2d^2}\right)+2\ln\left(\dfrac{r}{e}\right)\right\}+C_3 \\ -\dfrac{E\alpha\left(T_b-T_a\right)}{2(1-\nu)\ln\left(\dfrac{b}{a}\right)}\left[\dfrac{2}{(2\nu-1)}\left\{\ln\left(\dfrac{d}{a}\right)+\dfrac{1}{2}-\dfrac{e^2}{2d^2}\right\}+2\ln\left(\dfrac{r}{e}\right)\right] \\ -\dfrac{2E\alpha T_a}{(2\nu-1)}-\dfrac{2E\varepsilon_o}{(1-2\nu)} \end{array}\right]+T_a \qquad (3.52)$$

Elastic zone, $d \le r \le e$

$$T(r) = \left(\frac{1-\nu}{E\alpha}\right)\left[\begin{array}{l} k_1\sigma_Y\left\{1+\ln(a)\right\}+C_3-\dfrac{2E\alpha T_a}{(2\nu-1)} \\ -\dfrac{E\alpha(T_b-T_a)}{2(1-\nu)\ln\left(\dfrac{b}{a}\right)}\left\{\dfrac{2}{(2\nu-1)}\left\{\ln\left(\dfrac{d}{a}\right)+\dfrac{1}{2}-\dfrac{e^2}{2d^2}\right\}\right\} \\ -\dfrac{2k_1\sigma_Y}{(2\nu-1)}\left(1+\dfrac{e^2}{2d^2}\right)-\dfrac{2E\varepsilon_o}{(1-2\nu)} \end{array}\right]+T_a \qquad (3.53)$$

The analytical equivalent temperature fields in the Plastic zone I and II during second stage of plastic deformation is still given by Eqs. (3.48) and (3.49), where the values of the constants are different due to change of boundary conditions.

3.4 Numerical Results and Discussion

To exemplify the analytical model developed in Section 3.3 for the equivalent temperature field to imitate the original thermal autofrettage induced residual stress field in cylinder, an SS304 cylinder with the following radial dimensions is considered: inner radius a=10 mm and outer radius b=30 mm. The material properties of SS304 are presented in Table 3.1. To achieve thermal autofrettage in the current SS304 cylinder, the

`

different geometrical and loading parameters as obtained in Ref [9] are taken and summarized in Table 3.2.

Table 3.1 Material Properties of SS304

Density, ρ (kg/m^3)	Young's Modulus of Elasticity, E (GPa)	Poisson's ratio, v	Yield stress, σ_Y (MPa)	Coefficient of thermal expansion, α (/ ºC)
8000	193	0.30	205	17.2×10^{-6}

Table 3.2 Geometry and loading parameters in the thermal autofrettage of SS304 cylinder [9]

Radius of plastic-plastic interface, c (mm)	Radius of elastic-plastic interface, d (mm)	Temperature at the inner wall, T_a (ºC)	Autofrettage temperature difference, ($T_b - T_a$) (ºC)
11.9775	12.9193	25	120

3.4.1 Evaluation of equivalent temperature field

For the present autofrettage temperature difference induced in the SS304 cylinder, the cylinder is subjected to first stage of plastic deformation during thermal autofrettage. Thus, the equivalent temperature field in the cylinder in the two consecutive inner plastic zones and in the outer elastic zone are evaluated using Eqs. (3.48) – (3.50). The distribution of the equivalent temperature field for imitating the residual stress field in the thermally autofrettaged SS304 cylinder as a function of radius is shown in Fig. 3.2. It is observed that the equivalent temperature field decreases up to the radius of elastic-plastic interface d and then it becomes constant in the elastic zone.

`

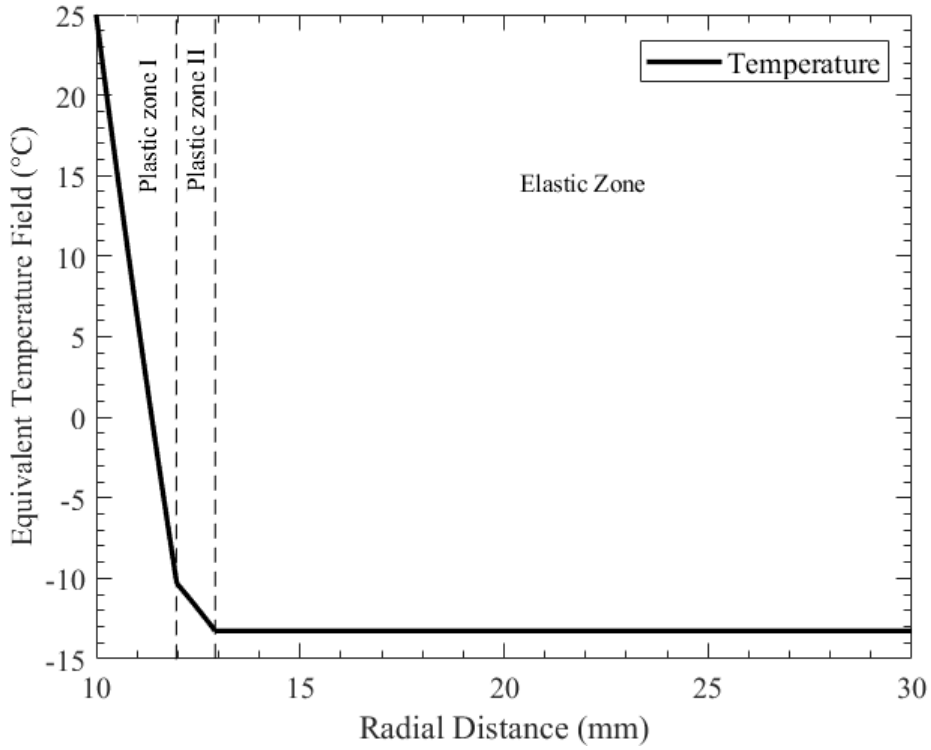

Fig. 3.2 The equivalent temperature field for imitating the original residual stresses induced by thermal autofrettage in SS304 Cylinder

3.4.2 Corroboration of the residual stress field induced by the equivalent temperature in the FEM model with the original thermal autofrettage induced residual stresses

In this section, the residual stress distribution in the SS304 cylinder is evaluated by applying the equivalent temperature field obtained in Subsection 3.4.1 in a two-dimensional FEM model and are corroborated with the original thermal autofrettage induced residual stress field due to Kamal and Dixit's model [9]. The FEM modelling is carried out using ABAQUS finite element package.

For the FEM analysis, the cross section of the cylinder with inner and outer radii 10 mm and 30 mm respectively is considered with the centre at the origin of a polar coordinate system. The geometry is meshed by using CPEG4R 4-noded bilinear generalized plane strain element of size 0.2 mm. A typical meshed geometry is shown in Fig 3.3. The meshing was done using sweep method. The number of nodes and elements used in the present model are 63226 and 62600, respectively. The equivalent temperature field obtained from Fig. 3.2 were applied on each and every radial node corresponding to

`

each radial distance. The displacement boundary conditions were imposed to solve the FEM model. The displacement in the *r*-direction at a node in the inner radius is constrained (u_r=0) and a node at the outer boundary of the cylindrical cross-section is fixed, *i.e.*, the displacements of the node both in the *r* and θ-directions are fixed (u_r=0, u_θ=0). The FEM model is then solved to obtain the radial, hoop and axial stress distributions.

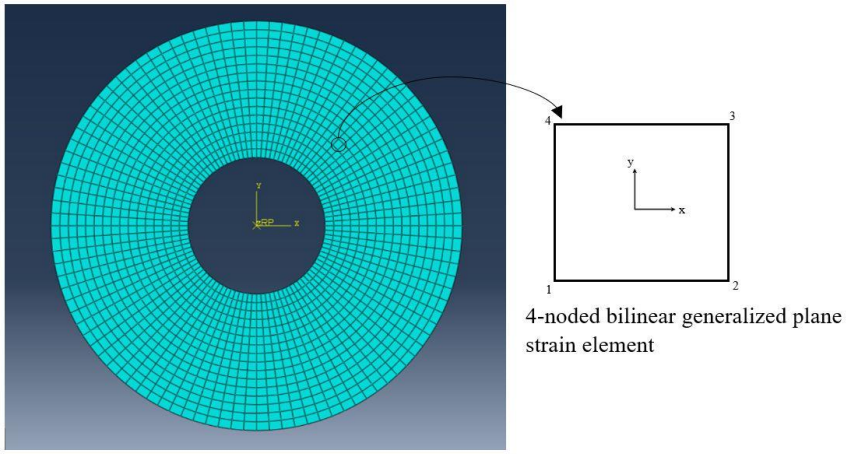

Fig. 3.3 A typical meshed geometry

The FEM stress solutions obtained by incorporating the equivalent temperature field are corroborated with the residual stress field originally induced by the method of thermal autofrettage using the solutions of Kamal and Dixit [9]. The corroboration of equivalent temperature field generated residual radial, hoop and axial stresses with the original thermal autofrettage induced residual stresses are shown in Figs. 3.4 (a), (b) and (c), respectively. It is observed that all the components of the residual stress fields obtained from FEM model is matching well with the original analytical generalized plane strain thermal autofrettage residual stress field. Thus, the analytical model for the equivalent temperature field developed in Section 3.3 is capable of reproducing the residual stress field induced by thermal autofrettage in cylinders with reasonable accuracy.

`

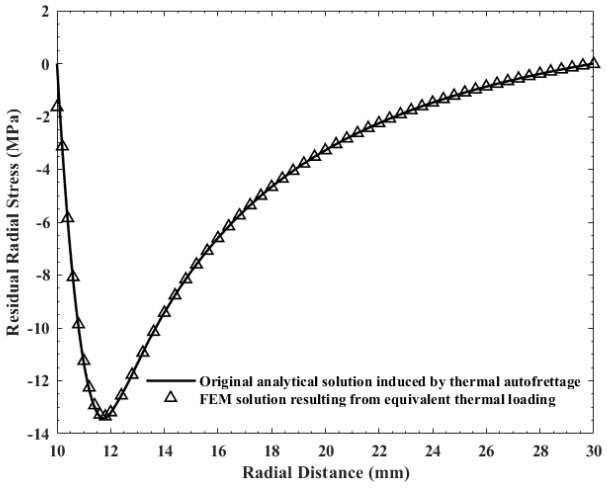

(a)

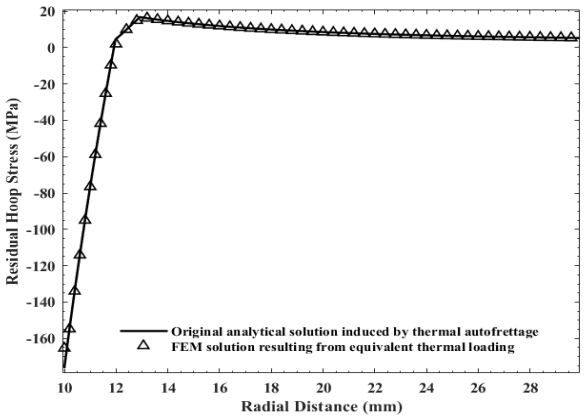

(b)

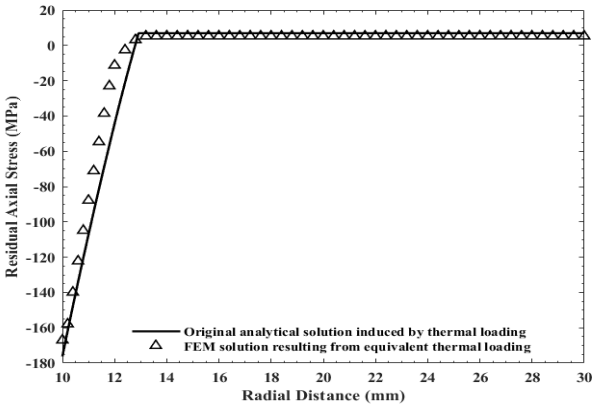

(c)

Fig. 3.4 Comparison of residual (a) radial, (b) hoop and (c) axial stress in the thermal autofrettage resulting from analytical solutions and present FEM solution due to equivalent temperature field

`

3.5 Conclusion

An analytical model for the equivalent temperature field to imitate the residual stresses induced by thermal autofrettage in cylinders is developed. The general expression of the equivalent temperature field can be used to evaluate the equivalent temperature field at every radial position if the residual stresses due to an analytical model or discrete numerical values of the residual stresses as a function of radii are known. In the present chapter, the closed-form analytical solutions for the equivalent temperature fields in cylinders due to thermal autofrettage are obtained using the known analytical expressions of residual stresses developed by Kamal and Dixit [9]. The methodology is numerically exemplified for a typical SS304 cylinder subjected to thermal autofrettage. It is observed that the present analytical solutions of equivalent temperature field incorporated in a finite element model can reproduce the original residual stress field induced by thermal autofrettage with reasonable accuracy.

`

Chapter 4

Epilogue

4.1 Conclusion

In this work, the evaluation of equivalent temperature field to emulate the residual stress field in a long hollow thick-walled cylinder induced by thermal autofrettage for application in a finite element method analysis is insinuated. The contribution of the present work is highlighted in the following:

- Development of an analytical model to imitate the original thermal autofrettage induced residual stresses in cylinders.
- Demonstration of the present methodology of applying equivalent temperature field in a typical SS304 cylinder in a two-dimensional FEM modelling using ABAQUS.
- Corroboration of the equivalent temperature field induced residual stresses with the original thermal autofrettage induced residual stresses.

It has been observed from the present work that the developed analytical solution for the equivalent temperature field can replicate the residual stresses induced by thermal autofrettage in the cylinder with reasonable accuracy. The findings of this work will help in studying the fatigue crack growth and subsequently in the evaluation of fatigue life of thermally autofrettaged cylinder numerically.

4.2 Scope for future work

There are several scopes to work in the area of thermal autofrettage. Some of the important research directions are highlighted below:

- Use of the present equivalent temperature field solution in studying crack-growth and fatigue life estimation in a finite element framework for thermally autofrettaged thick-walled cylinder.
- Crack-propagation in thermally autofrettaged cylinder using different crack geometries and the effect of multiple cracking.

`

- Autofrettage of components other than cylindrical or spherical.
- Refinement of analytical modelling of thermal autofrettage using more realistic yield criterion such as von Mises yield criterion.
- Studying reverse yielding in thermally autofrettaged cylinder.

`

Nomenclature

a = inner radius of the cylinder

b = outer radius of the cylinder

C_1, C_2, C_3, C_5, C_6, C_7 = integration constants

c, f = radii of plastic-plastic interface

d, e = radii of elastic-plastic interface

E = Young's modulus of elasticity

k_1 = sign factor

p_i = internal working pressure

r = radius of cylinder

T_a = temperature at the inner surface of the cylinder

T_b = temperature at the outer surface of the cylinder

Greek Symbols

α = coefficient of thermal expansion

$\varepsilon_\circ$ = constant axial strain

ν = Poisson's Ratio

σ_r = radial stress

σ_Y = yield stress

σ_z = axial stress

σ_θ = hoop stress

$(\sigma_r)_{res}$ = residual radial stress

$(\sigma_z)_{res}$ = residual axial stress

$(\sigma_\theta)_{res}$ = residual hoop stress

`

`

References

[1] M. A. Malik, S. Khushnood, A REVIEW OF SWAGE-AUTOFRETTAGE PROCESS, *The Proceedings of the International Conference on Nuclear Engineering (ICONE)*, The Japan Society of Mechanical Engineers, *63*, 2003.

[2] M.C. Gibson, Determination of residual stress distributions in autofrettaged thick-walled cylinders, Ph.D. Thesis, Defence College of Management and Technology, Cranfield University, U.K., 2008.

[3] T. E. Davidson, C. S. Barton, A. N. Reiner, D. P. Kendall, New approach to the autofrettage of high-strength cylinders: An oversize mandrel is forced through a 4340-steel tube to plastically deform the walls and, thereby, produce favourable residual stress patterns, *Experimental Mechanics*, *2*, 33-40, 1962.

[4] A. R. T. H. U. R. A. Erza, W. Howell, H. Glick, M. Kaplan, *U.S. Patent No. 3,751,954*. Washington, DC: U.S. Patent and Trademark Office, 1973.

[5] D. G. B. Thomas, The autofrettage of thick tubes with free ends, *Journal of the Mechanics and Physics of Solids*, *1*(2), 124-133, 1953.

[6] B. Avitzur, Autofrettage—Stress distribution under load and retained stresses after depressurization, *International journal of pressure vessels and piping*, *57*(3), 271-287, 1994.

[7] D. W. A. Rees, A theory of autofrettage with applications to creep and fatigue, *International journal of pressure vessels and piping*, *30*(1), 57-76, 1987.

[8] A. P. Parker, Autofrettage of open-end tubes—pressures, stresses, strains, and code comparisons, *J. Pressure Vessel Technol.*, *123*(3), 271-281, 2001.

[9] S. M. Kamal, U. S. Dixit, Feasibility study of thermal autofrettage of thick-walled cylinders, *Journal of Pressure Vessel Technology*, *137*(6), 2015.

[10] H. R. Zare, H. Darijani, A novel autofrettage method for strengthening and design of thick-walled cylinders, *Materials & Design*, *105*, 366-374, 2016.

`

[11] S. M. Kamal, U. S. Dixit, Feasibility study of thermal autofrettage process, *Advances in Material Forming and Joining: 5th International and 26th All India Manufacturing Technology, Design and Research Conference, AIMTDR 2014*, Springer India, 81-107, 2015.

[12] M. A. Hussain, S. L. Pu, J. D. Vasilakis, P. O'Hara, Simulation of Partial Autofrettage by Thermal Loads, *ASME J. Pressure Vessel Technology*, *102*(3), 314–318, 1980.

[13] A. Stacey, H.J. MacGillivary, G.A. Webster, P.J. Webster, K.R.A. Ziebeck, Measurement of residual stresses by neutron diffraction, *Journal of Strain Analysis for Engineering Design*, *20*(2), 93−100, 1985.

[14] W. S. Shim, J. H. Kim, Y. S. Lee, K. U. Cha, S. K. Hong, Hydraulic autofrettage of thick-walled cylinders incorporating Bauschinger effect, *Experimental Mechanics*, *50*, 621–626, 2010.

[15] S. Alexandrov, W. Jeong, K. Chung, Descriptions of reversed yielding in internally pressurized tubes, *ASME Journal of Pressure Vessel Technology*, *138*, 2016.

[16] Y. Ma, S. Y. Zhang, J. Yang, P. Zhang, Neutron diffraction, finite element and analytical investigation of residual strains of autofrettaged thick-walled pressure vessels, *International Journal of Pressure Vessels and Piping*, *200*, 2022.

[17] M.J. Iremonger, G.S. Kalsi, A numerical study of swage autofrettage, *ASME Journal of Pressure Vessel Technology*, *125*, 347-351, 2003.

[18] M.C. Gibson, A. Hameed, J.G. Hetherington, Investigation of residual stress development during swage autofrettage, using finite element analysis, *ASME Journal of Pressure Vessel Technology*, *136*, 2014

[19] Z. Hu, A.P. Parker, Implementation and validation of true material constitutive model for accurate modelling of thick-walled cylinder swage autofrettage, *International Journal of Pressure Vessels and Piping*, *191*, 2021.

[20] T.E. Davidson, D.P. Kendall, A.N. Reiner, Residual stresses in thick-walled cylinders resulting from mechanically induced overstrain, *Experimental Mechanics*, *3*, 253–262, 2021.

[21] S. M. Kamal, U. S. Dixit, A. Roy, Q. Liu, V. V. Silberschmidt, Comparison of plane-stress, generalized-plane-strain and 3D FEM elastic–plastic analyses of thick-walled

`

cylinders subjected to radial thermal gradient, *International Journal of Mechanical Sciences*, *131*, 744-752, 2017.

[22] S. M. Kamal, A. C. Borsaikia, U. S. Dixit, Experimental assessment of residual stresses induced by the thermal autofrettage of thick-walled cylinders, *The Journal of Strain Analysis for Engineering Design*, *51*(2), 144-160, 2016.

[23] S. M. Kamal, A. C. Borsaikia, U. S. Dixit, Measurement of residual stresses in thermally autofrettaged thickwalled cylinders, *Proceedings of the 30th National Convention of Production Engineers*, 18-19, 2015.

[24] S. M. Kamal, M. Perl, D. Bharali, "Generalized Plane Strain Study of Rotational Autofrettage of Thick-Walled Cylinders—Part I: Theoretical Analysis.", ASME. *J. Pressure Vessel Technol*, *141*(5), 2019.

[25] S. M. Kamal, M. Perl, "Generalized Plane Strain Study of Rotational Autofrettage of Thick-Walled Cylinders—Part II: Numerical Evaluation.", ASME. *J. Pressure Vessel Technol*., *141*(5), 2019.

[26] S. M. Kamal, Analysis of Residual Stress in the Rotational Autofrettage of Thick-Walled Disks. *Journal of Pressure Vessel Technology*, *140*, 2018.

[27] R. Shufen, U. S. Dixit, Effect of length in rotational autofrettage of long cylinders with free ends, *Proceedings of the Institution of Mechanical Engineers, Part C: Journal of Mechanical Engineering Science*, *236*(6), 2981-2994, 2022.

[28] S. M. Kamal, U. S. Dixit, A comparative study of thermal and hydraulic autofrettage, *Journal of Mechanical Science and Technology*, *30*, 2483-2496, 2016.

[29] S. M. Kamal, U. S. Dixit, Enhancement of fatigue life of thick-walled cylinders through thermal autofrettage combined with shrink-fit, *Strengthening and Joining by Plastic Deformation: Select Papers from AIMTDR 2016*, 1-30, 2019.

[30] S. M. Kamal, U. S. Dixit, Fatigue Life Enhancement of Thermally Autofrettaged Cylinders through Shrink-Fit, 2016

[31] S. M. Kamal, U. S. Dixit, Q. Liu, V. V. Silberschmidt, A. Roy, Thermo-Elasto-Plastic Finite Element Stress Analysis of Thick-Walled Cylinder and its Comparison with Plane Stress and Plane Strain Analyses.

`

[32] S. M. Kamal, A. C. Borsaikia, U. S. Dixit, Experimental assessment of residual stresses induced by the thermal autofrettage of thick-walled cylinders, *The Journal of Strain Analysis for Engineering Design*, *51*(2), 144-160, 2016.

[33] R. Shufen, U. S. Dixit, A finite element method study of combined hydraulic and thermal autofrettage process, *Journal of Pressure Vessel Technology*, *139*(4), 2017

[34] R. Shufen, U. S. Dixit, An analysis of thermal autofrettage process with heat treatment, *International Journal of Mechanical Sciences*, *144*, 134-145, 2018.

[35] R. Shufen, N. Mahanta, U. S. Dixit, Development of a thermal autofrettage setup to generate compressive residual stresses on the surfaces of a cylinder, *Journal of Pressure Vessel Technology*, *141*(5), 2019.

[36] Mohit Rajput, S.M. Kamal, R.U. Patil, Estimation of the residual stresses in thermal autofrettage of hollow disk using von Mises yield criterion, *Proceedings of the 67th Congress of the Indian Society of Theoretical and Applied Mechanics (ISTAM) (An International Conference)*, 2022.

[37] R. Hill, The Mathematical Theory of Plasticity, Clarendon Press, Oxford, UK, 1950.

[38] A. P. Parker, J. R. Farrow, On the equivalence of axisymmetric bending, thermal, and autofrettage residual stress fields, *The Journal of Strain Analysis for Engineering Design*, *15*(1), 51-52, 1980.

[39] S. L. Pu, M. A. Hussain, Residual stress redistribution caused by notches and cracks in a partially autofrettaged tube, *ASME J. Pressure Vessel Technology*, *103*(4), 302-306, 1981.

[40] M. Perl, The temperature field for simulating partial autofrettage in an elasto-plastic thick-walled cylinder, *ASME J. Pressure Vessel Technology*, *110*(1), 100-102, 1988.

[41] M. Perl, Thermal simulation of an arbitrary residual stress field in a fully or partially autofrettaged thick-walled spherical pressure vessel, *Journal of pressure vessel technology*, *130*(3), 2008.

[42] M. Perl, R. Arone, Stress Intensity Factors for a Radially Multicracked Partially-Autofrettaged Pressurized Thick-Walled Cylinder, *ASME J. Pressure Vessel Technol.*, *110*(2), 147–154, 1988.

`

[43] M. Perl, M. Steiner, The Beneficial Effect of Full or Partial Autofrettage on the Combined 3-D Stress Intensity Factor for an Inner Radial Lunular or Crescentic Crack in a Spherical Pressure Vessel, *Eng. Fract. Mech., 156*, 124–140, 2016.

[44] M. Perl, M. Steiner, The Beneficial Effect of Full or Partial Autofrettage on the Combined 3-D Stress Intensity Factors for Inner Radial Crack Arrays in a Spherical Pressure Vessel, Eng. Fract. Mech., *175*, 46–56, 2017.

[45] R. R. de Swardt, Finite Element Simulation of Crack Compliance Experiments to Measure Residual Stresses in Thick-Walled Cylinders, *ASME J. Pressure Vessel Technol*., *125*(3), 305–308, 2003.

[46] U. Güven, Generalized Equivalent Temperature Fields of Thick Walled Pressure Vessels, *Meccanica, 47*(5), 1307–1311, 2012.

[47] M. Pearl, S. M. Kamal, S. Mulera, The Use of an Equivalent Temperature Field to Emulate an Induced Residual Stress Field in a Rotating Disk Due to Full or Partial Rotational Autofrettage, *Journal of Pressure Vessel Technology*, *144*(6), 2022.

[48] J. Chakrabarty, Theory of Plasticity, 3rd ed., Butterworth-Heinemann, Burlington, Canada, 2006.

[49] S. P. Timoshenko, J. N. Goodier, Theory of Elasticity,3rd ed., McGraw-Hill, New York, 1970.

`

`

Appendix

Expressions of different constants involved in equations presented in Section 3.2 of Chapter 3

$$C_3 = R + \left[\begin{array}{l} \dfrac{2\nu b^2 c^{-1+\sqrt{2(1-\nu)}}}{(2\nu-1)\left\{b^2+d^2(2\nu-1)\right\}} d^{1-\sqrt{2(1-\nu)}} \left\{ \dfrac{1-\nu+\nu\sqrt{2(1-\nu)}}{2\nu\sqrt{2(1-\nu)}} \right\} \\ -\dfrac{2\nu b^2 c^{-1-\sqrt{2(1-\nu)}}}{(2\nu-1)\left\{b^2+d^2(2\nu-1)\right\}} \left\{ \dfrac{1-\nu-\nu\sqrt{2(1-\nu)}}{d^{-1-\sqrt{2(1-\nu)}} 2\nu\sqrt{2(1-\nu)}} \right\} - \dfrac{1}{(2\nu-1)} \end{array} \right] E\varepsilon_o, \tag{A.1}$$

$$C_5 = Q + \frac{2\nu b^2}{(2\nu-1)\left\{b^2+d^2(2\nu-1)\right\}} d^{1-\sqrt{2(1-\nu)}} \times \left\{ \frac{1-\nu+\nu\sqrt{2(1-\nu)}}{2\nu\sqrt{2(1-\nu)}} \right\} E\varepsilon_o, \tag{A.2}$$

$$C_6 = P - \frac{2\nu b^2}{(2\nu-1)\left\{b^2+d^2(2\nu-1)\right\}} \times \left\{ \frac{1-\nu-\nu\sqrt{2(1-\nu)}}{d^{-1-\sqrt{2(1-\nu)}} 2\nu\sqrt{2(1-\nu)}} \right\} E\varepsilon_o, \tag{A.3}$$

$$R = Qc^{-1+\sqrt{2(1-\nu)}} - k_1\sigma_Y \ln c + Pc^{-1-\sqrt{2(1-\nu)}} + \frac{k_1\sigma_Y}{(2\nu-1)} + \frac{E\alpha T_a}{(2\nu-1)} + \frac{E\alpha(T_b-T_a)}{(2\nu-1)\ln\left(\frac{b}{a}\right)} \ln\left(\frac{c}{a}\right) - \frac{2E\alpha(T_b-T_a)}{(2\nu-1)^2 \ln\left(\frac{b}{a}\right)} - \frac{E\alpha(T_b-T_a)}{(2\nu-1)\ln\left(\frac{b}{a}\right)}, \tag{A.4}$$

$$Q = -Pd^{-2\sqrt{2(1-\nu)}} \left\{ \frac{1-\nu+\nu\sqrt{2(1-\nu)}}{1-\nu-\nu\sqrt{2(1-\nu)}} \right\} - \frac{E\alpha(T_b-T_a)}{(2\nu-1)\ln\left(\frac{b}{a}\right)} \frac{1+\upsilon}{d^{-1+\sqrt{2(1-\nu)}} \left\{1-\nu-\nu\sqrt{2(1-\nu)}\right\}}, \tag{A.5}$$

`

$$P=\frac{E\alpha\left(T_b-T_a\right)}{\left(2\nu-1\right)\ln\left(\frac{b}{a}\right)}\left\{\frac{1-\nu-\nu\sqrt{2\left(1-\nu\right)}}{d^{-1-\sqrt{2(1-\nu)}}2\nu\sqrt{2\left(1-\nu\right)}}\right\}\left\{\begin{array}{l}\ln\left(\frac{d}{a}\right)-\\ \frac{2\nu+1}{2\nu-1}-\frac{1+\nu}{1-\nu-\nu\sqrt{2\left(1-\nu\right)}}\end{array}\right\}$$

$$-\frac{E\alpha\left(T_b-T_a\right)}{2\left(1-\nu\right)\ln\left(\frac{b}{a}\right)}\left\{\frac{1-\nu-\nu\sqrt{2\left(1-\nu\right)}}{d^{-1-\sqrt{2(1-\nu)}}2\nu\sqrt{2\left(1-\nu\right)}}\right\}\left[\begin{array}{l}\ln\left(\frac{b}{d}\right)+\\ \left\{\frac{b^2-d^2}{b^2+d^2\left(2\nu-1\right)}\right\}\left\{\ln\left(\frac{b}{a}\right)\left(2\nu-1\right)-\nu-\ln\left(\frac{d}{a}\right)\right\}\end{array}\right] \quad \text{(A.6)}$$

$$+\frac{2\nu b^2}{\left(2\nu-1\right)\left\{b^2+d^2\left(2\nu-1\right)\right\}}\left\{\frac{1-\nu-\nu\sqrt{2\left(1-\nu\right)}}{d^{-1-\sqrt{2(1-\nu)}}2\nu\sqrt{2\left(1-\nu\right)}}\right\}k_1\sigma_Y$$

$$+\frac{2\nu b^2}{\left(2\nu-1\right)\left\{b^2+d^2\left(2\nu-1\right)\right\}}\left\{\frac{1-\nu-\nu\sqrt{2\left(1-\nu\right)}}{d^{-1-\sqrt{2(1-\nu)}}2\nu\sqrt{2\left(1-\nu\right)}}\right\}E\alpha T_a,$$

$$\varepsilon_o=\frac{k_1\sigma_Y}{AE}\left\{\ln c\frac{c^2}{2}-\ln a\frac{a^2}{2}+\frac{1}{4}\left(c^2-a^2\right)+\frac{\nu\left(d^2-c^2\right)}{2\nu-1}+\frac{\nu d^2\left(b^2-d^2\right)}{b^2+d^2\left(2\nu-1\right)}\right\}+\frac{R}{AE}\left(\frac{c^2-a^2}{2}\right)$$

$$+\frac{Q}{AE}\left\{\frac{d^{1+\sqrt{2(1-\nu)}}-c^{1+\sqrt{2(1-\nu)}}}{1+\sqrt{2\left(1-\nu\right)}}\right\}+\frac{P}{AE}\left\{\frac{d^{1-\sqrt{2(1-\nu)}}-c^{1-\sqrt{2(1-\nu)}}}{1-\sqrt{2\left(1-\nu\right)}}\right\}+\frac{\alpha T_a}{A}\left[\begin{array}{l}\frac{d^2-c^2}{2\left(2\nu-1\right)}-\\ \frac{\left(b^2-d^2\right)^2}{2\left\{b^2+d^2\left(2\nu-1\right)\right\}}\end{array}\right]$$

$$+\frac{\alpha\left(T_b-T_a\right)}{\left(2\nu-1\right)\ln\left(\frac{b}{a}\right)A}\left\{\ln\left(\frac{d}{a}\right)\frac{d^2}{2}-\ln\left(\frac{c}{a}\right)\frac{c^2}{2}-\frac{1}{2}\left(d^2-c^2\right)\frac{6\nu+1}{2\left(2\nu-1\right)}\right\}$$

$$+\frac{\alpha\left(T_b-T_a\right)}{2\left(1-\nu\right)\ln\left(\frac{b}{a}\right)A}\left[\begin{array}{l}-\nu d^2\ln\left(\frac{b}{d}\right)-\left\{\frac{\nu d^2\left(b^2-d^2\right)}{b^2+d^2\left(2\nu-1\right)}\right\}\left\{\ln\left(\frac{b}{a}\right)\left(2\nu-1\right)-\nu-\ln\left(\frac{d}{a}\right)\right\}\\ -2\left(1-\nu\right)\left\{\ln\left(\frac{b}{a}\right)\frac{b^2}{2}-\ln\left(\frac{d}{a}\right)\frac{d^2}{2}-\frac{1}{4}\left(b^2-d^2\right)\right\}\end{array}\right], \quad \text{(A.7)}$$

`

$$A=\frac{d^2-c^2}{2(2\nu-1)}-\frac{\left(b^2-d^2\right)^2}{2\left\{b^2+d^2(2\nu-1)\right\}}$$
$$-\left(\frac{c^2-a^2}{2}\right)\left\{\begin{array}{l}\dfrac{2\nu b^2}{(2\nu-1)\left\{b^2+d^2(2\nu-1)\right\}2\sqrt{2(1-\nu)}}\left(\begin{array}{l}\left(\dfrac{c}{d}\right)^{-1+\sqrt{2(1-\nu)}}\left(\begin{array}{l}1-\nu\\+\nu\sqrt{2(1-\nu)}\end{array}\right)\\-\left(\dfrac{c}{d}\right)^{-1-\sqrt{2(1-\nu)}}\left(\begin{array}{l}1-\nu-\\\nu\sqrt{2(1-\nu)}\end{array}\right)\end{array}\right)-\\\dfrac{1}{(2\nu-1)}\end{array}\right\}$$
$$-\left\{\frac{d^{1+\sqrt{2(1-\nu)}}-c^{1+\sqrt{2(1-\nu)}}}{1+\sqrt{2(1-\nu)}}\right\}\frac{2\nu b^2}{(2\nu-1)\left\{b^2+d^2(2\nu-1)\right\}}d^{1-\sqrt{2(1-\nu)}}\left\{\frac{1-\nu+\nu\sqrt{2(1-\nu)}}{2\nu\sqrt{2(1-\nu)}}\right\}$$
$$+\left\{\frac{d^{1-\sqrt{2(1-\nu)}}-c^{1-\sqrt{2(1-\nu)}}}{1-\sqrt{2(1-\nu)}}\right\}\frac{2\nu b^2}{(2\nu-1)\left\{b^2+d^2(2\nu-1)\right\}}\left\{\frac{1-\nu-\nu\sqrt{2(1-\nu)}}{d^{-1-\sqrt{2(1-\nu)}}2\nu\sqrt{2(1-\nu)}}\right\}. \tag{A.8}$$

$$C_7=M+\frac{E\varepsilon_o}{(1-2\nu)}, \tag{A.9}$$

$$M=\frac{E\alpha T_a}{(2\nu-1)}+\frac{E\alpha\left(T_b-T_a\right)}{2(1-\nu)\ln\left(\frac{b}{a}\right)}$$
$$\times\left[\frac{1}{(2\nu-1)}\left\{\ln\left(\frac{d}{a}\right)+\frac{1}{2}-\frac{e^2}{2d^2}\right\}-\ln\left(\frac{e}{a}\right)\right] \tag{A.10}$$
$$+\left\{\frac{1}{(2\nu-1)}\left(1+\frac{e^2}{2d^2}\right)+\frac{1}{2}-\ln\left(\frac{f}{e}\right)+\ln f\right\}k_1\sigma_Y,$$

$$B=\left\{\frac{b^2-a^2}{2(2\nu-1)}\right\}, \tag{A.11}$$

$$C_5=-C_6d^{-2\sqrt{2(1-\nu)}}\left\{\frac{1-\nu+\nu\sqrt{2(1-\nu)}}{1-\nu-\nu\sqrt{2(1-\nu)}}\right\}-$$
$$\frac{E\alpha\left(T_b-T_a\right)}{(2\nu-1)\ln\left(\frac{b}{a}\right)}\frac{(1+\nu)}{d^{-1+\sqrt{2(1-\nu)}}\left\{1-\nu-\nu\sqrt{2(1-\nu)}\right\}}, \tag{A.12}$$

`

$$N = C_5 c^{-1+\sqrt{2(1-\nu)}} + C_6 c^{-1-\sqrt{2(1-\nu)}} + \frac{k_1\sigma_Y}{(2\nu-1)} + \frac{E\alpha T_a}{(2\nu-1)}$$
$$+ \frac{E\alpha(T_b - T_a)}{(2\nu-1)\ln\left(\frac{b}{a}\right)}\left\{\ln\left(\frac{c}{a}\right) - \frac{2\nu+1}{2\nu-1}\right\} - k_1\sigma_Y \ln c, \tag{A.13}$$

$$C_6 = \frac{E\alpha(T_b - T_a)}{(2\nu-1)\ln\left(\frac{b}{a}\right)}\left\{\frac{1-\nu-\nu\sqrt{2(1-\nu)}}{d^{-1-\sqrt{2(1-\nu)}}\,2\nu\sqrt{2(1-\nu)}}\right\}\left\{\ln\left(\frac{d}{a}\right) - \frac{2\nu+1}{2\nu-1} - \frac{(1+\nu)}{1-\nu-\nu\sqrt{2(1-\nu)}}\right\}$$
$$- \frac{E\alpha(T_b - T_a)}{2(1-\nu)\ln\left(\frac{b}{a}\right)}\left\{\frac{1-\nu-\nu\sqrt{2(1-\nu)}}{d^{-1-\sqrt{2(1-\nu)}}\,2\nu\sqrt{2(1-\nu)}}\right\}\left[\frac{1}{(2\nu-1)}\left\{\ln\left(\frac{d}{a}\right) + \frac{1}{2} - \frac{e^2}{2d^2}\right\} - \ln\left(\frac{d}{a}\right) + \frac{1}{2} - \frac{e^2}{2d^2}\right]$$
$$- \left\{\frac{1-\nu-\nu\sqrt{2(1-\nu)}}{d^{-1-\sqrt{2(1-\nu)}}\,2\nu\sqrt{2(1-\nu)}}\right\}\left(\frac{2\nu}{2\nu-1}\right)k_1\sigma_Y\frac{e^2}{2d^2},$$

(A.14)

$$\varepsilon_o = \frac{k_1\sigma_Y}{BE}\left[\begin{array}{l}\ln c\left(\frac{c^2}{2}\right) - \ln a\left(\frac{a^2}{2}\right) + \frac{1}{4}(c^2-a^2) + \frac{\nu}{2\nu-1}(d^2-c^2) + \frac{\nu}{2\nu-1}(f^2-d^2)\left(1+\frac{e^2}{2d^2}\right)\\ -\nu\left\{\ln\left(\frac{f}{e}\right)f^2 - \frac{1}{2}(f^2-e^2)\right\} - \frac{1}{4}(b^2-f^2) - \ln b\left(\frac{b^2}{2}\right) + \ln f\left(\frac{f^2}{2}\right)\end{array}\right]$$
$$+ \frac{N}{2BE}(c^2-a^2) + \frac{C_5}{BE}\left\{\frac{d^{1+\sqrt{2(1-\nu)}} - c^{1+\sqrt{2(1-\nu)}}}{1+\sqrt{2(1-\nu)}}\right\} + \frac{C_6}{BE}\left\{\frac{d^{1-\sqrt{2(1-\nu)}} - c^{1-\sqrt{2(1-\nu)}}}{1-\sqrt{2(1-\nu)}}\right\}$$
$$+ \frac{\alpha T_a}{2(2\nu-1)B}(f^2-c^2)$$
$$+ \frac{\alpha(T_b - T_a)}{(2\nu-1)\ln\left(\frac{b}{a}\right)B}\left\{\ln\left(\frac{d}{a}\right)\frac{d^2}{2} - \ln\left(\frac{c}{a}\right)\frac{c^2}{2} - \frac{3}{4}(d^2-c^2) - \frac{d^2-c^2}{2\nu-1}\right\} + \frac{M}{2BE}(b^2-f^2)$$
$$+ \frac{\alpha(T_b - T_a)}{2(1-\nu)\ln\left(\frac{b}{a}\right)B}\left[\begin{array}{l}\frac{\nu}{(2\nu-1)}\left\{\ln\left(\frac{d}{a}\right) + \frac{1}{2} - \frac{e^2}{2d^2}\right\}(f^2-d^2) -\\ \left\{\ln\left(\frac{e}{a}\right)e^2 - \ln\left(\frac{d}{a}\right)d^2 - \frac{1}{2}(e^2-d^2)\right\}\\ +\nu\left\{\ln\left(\frac{f}{e}\right)f^2 - \frac{1}{2}(f^2-e^2)\right\} - \left\{\ln\left(\frac{f}{a}\right)f^2 - \ln\left(\frac{e}{a}\right)e^2 - \frac{1}{2}(f^2-e^2)\right\}\end{array}\right].$$

(A.15)